Stem Cell Reports
Resource
ISSCR
OPEN ACCESS

Transcriptomically Guided Mesendoderm Induction of Human Pluripotent Stem Cells Using a Systematically Defined Culture Scheme

Richard L. Carpenedo,[1,2,*] Sarah Y. Kwon,[1,7] R. Matthew Tanner,[1,2,3] Julien Yockell-Lelièvre,[1] Chandarong Choey,[1,8] Carole Doré,[1] Mirabelle Ho,[1] Duncan J. Stewart,[1,4] Theodore J. Perkins,[1,5,6] and William L. Stanford[1,2,3,6,*]

[1]The Sprott Centre for Stem Cell Research, Regenerative Medicine Program, Ottawa Hospital Research Institute, Ottawa, ON, Canada
[2]Ottawa Institute of Systems Biology, Ottawa, ON, Canada
[3]Department of Cellular and Molecular Medicine, University of Ottawa, Ottawa, ON, Canada
[4]Sinclair Centre for Regenerative Medicine, Ottawa Hospital Research Institute, Ottawa, ON, Canada
[5]Ottawa Bioinformatics Core Facility, Ottawa Hospital Research Institute, Ottawa, ON, Canada
[6]Department of Biochemistry, Microbiology, and Immunology, University of Ottawa, Ottawa, ON, Canada
[7]Present address: Center for Commercialization of Regenerative Medicine, 661 University Avenue, Toronto, ON, Canada
[8]Present address: Sick Kids-UHN Flow and Mass Cytometry Facility, Toronto, ON, Canada
*Correspondence: rcarpenedo@ohri.ca (R.L.C.), wstanford@ohri.ca (W.L.S.)
https://doi.org/10.1016/j.stemcr.2019.11.001

SUMMARY

Human pluripotent stem cells (hPSCs) are an essential cell source in tissue engineering, studies of development, and disease modeling. Efficient, broadly amenable protocols for rapid lineage induction of hPSCs are of great interest in the stem cell biology field. We describe a simple, robust method for differentiation of hPSCs into mesendoderm in defined conditions utilizing single-cell seeding (SCS) and BMP4 and Activin A (BA) treatment. BA treatment was readily incorporated into existing protocols for chondrogenic and endothelial progenitor cell differentiation, while fine-tuning of BA conditions facilitated definitive endoderm commitment. After prolonged differentiation *in vitro* or *in vivo*, BA pretreatment resulted in higher mesoderm and endoderm levels at the expense of ectoderm formation. These data demonstrate that SCS with BA treatment is a powerful method for induction of mesendoderm that can be adapted for use in mesoderm and endoderm differentiation.

INTRODUCTION

Pluripotent stem cells (PSCs) are a powerful tool in a variety of applications ranging from basic studies of development and disease to cell-based therapeutics and regenerative medicine applications (Evans and Kaufman, 1981; Martin, 1981; Reubinoff et al., 2000). Human embryonic stem cells (hESCs) (Thomson et al., 1998) and induced PSCs (iPSCs) (Takahashi et al., 2007; Yu et al., 2007) are two classes of PSCs that are particularly well-suited for modeling genetic diseases (Park et al., 2008; Soldner et al., 2009) as well as serving as a renewable cell source for tissue engineering purposes (Wu and Hochedlinger, 2011). For the potential of PSCs to be realized from basic science to clinical applications, efficient directed differentiation protocols to produce relevant cell types are required. While much work has been done in the area of inducing differentiation of PSCs to various types of somatic cells, methods for generating cells of interest that are simple, chemically defined, and can be adapted and optimized for many cell types are of great interest to a breadth of scientists, engineers, and clinicians.

A number of physical parameters influence hPSC differentiation, including cell density, colony size, and dissociation method, as hPSCs are exquisitely sensitive to paracrine factors from neighboring cells (Davey and Zandstra, 2006) and can undergo apoptosis and display karyotypic abnormalities when passaged as single cells (Draper et al., 2004; Mitalipova et al., 2005). Advanced microengineering approaches have been used to control cell spacing and colony size, resulting in differentiation platforms amenable to induction of multiple lineages (Bauwens et al., 2008; Lee et al., 2009; Martyn et al., 2019; Nazareth et al., 2013). Although microfabricated systems can be beneficial for enhancing microenvironmental control over differentiating cells, they are not practical for many laboratories performing fundamental studies. Thus, a simple and broadly applicable platform for controlling microenvironmental conditions that can be utilized in laboratories with a range of specialties to induce differentiation of human PSCs is required.

Here we describe a simple, versatile method to enhance differentiation of multiple mesodermal cells types with a brief pre-differentiation protocol. After 48 h of treatment with moderate concentrations of both BMP4 and Activin A (referred to as BA), a reduction of pluripotency genes and proteins was observed, concurrent with an upregulation of a mesendoderm gene signature. Integration of this 48-h treatment protocol into existing differentiation protocols enhanced the production of chondrocytes and endothelial progenitor cells while reducing neural differentiation capacity. Prolonged exposure of BA-treated cells to basal media without exogenous cues for 14 days resulted in single-cell gene expression profiles consistent

with mesoderm and endoderm induction. Teratomas formed from cells pretreated with BA consisted of a higher ratio of mesoderm and endoderm to ectoderm tissue than teratomas formed from untreated cells. Thus, our pre-differentiation system is a simple and effective means for production of mesendoderm progenitors and downstream mesodermal cell lineages.

RESULTS

Single-Cell Seeding in Defined Conditions Produces Robust Mesendoderm Differentiation

The addition of BA to basal medium has been shown to induce differentiation of hPSCs to a primitive streak/mesendoderm phenotype in standard colony-seeded cultures (Teo et al., 2012) and in a micropatterned colony culture system (Nazareth et al., 2013). We sought to approximate the rigorous spatial control afforded by the micropatterned system and the subsequent control over paracrine signaling effects while circumventing the microcontact printing step necessary to produce micropatterns. We hypothesized that the stricter control of initial cell density in single-cell seeding (SCS) would allow for more uniform and reproducible cell dispersions than colony seeding, which would in turn produce rapid and robust mesendoderm differentiation, similar to micropatterned cultures. To test this hypothesis, we assessed the spatial uniformity of cells seeded by colony and SCS methodologies as well as the downstream differentiation response.

Chemically defined, feeder-free conditions comprising Essential 8 (E8) medium (Chen et al., 2011) and Matrigel-coated dishes were used for hPSC maintenance to optimize hPSC homogeneity. After overnight colony seeding or SCS, H9 hESCs were stained with Hoechst (Figure 1A), and high-content imaging was used to assess the uniformity of cell seeding. Coefficient of variation (CV) for the number of cells in a 345 × 345-μm grid (equivalent to 25 grids in a 10× image) was calculated and normalized to the CV of an equal number of cells in a simulated random uniform distribution to assess uniformity of seeding. SCS resulted in significantly lower normalized CV than colony seeding across all densities evaluated ($p < 0.0001$), indicating a greater degree of spatial uniformity (Figure 1B). The colony split ratio and SCS density did not have a significant effect on spatial distribution when normalized to a uniform distribution of the same cell number, nor did the SCS density influence overnight cell seeding efficiency (~60%). Thus, SCS produced a spatially uniform cell distribution at a broad range of seeding densities.

We then reasoned that the enhanced uniformity of SCS would result in more robust mesendoderm differentiation compared with colony seeding. To test this hypothesis, H9 hESCs were seeded overnight in E8 as colonies (split 1:6) or single cells (1.5×10^5 cells/mL) and allowed to differentiate spontaneously via removal of transforming growth factor β (TGF-β) and fibroblast growth factor (FGF2) from E8 medium to produce a basal media known as E6, or were directed to mesendoderm by addition of BMP4 (40 ng/mL) and Activin A (40 ng/mL) to E6 medium (termed BA; schematically depicted in Figure 1C). SCS density and BA concentrations were chosen based on empirical testing of a range of densities (data not shown) and concentrations (Figures S1A and S1B) as well as previous literature (Nazareth et al., 2013). POU5F1 (OCT4) protein abundance was not significantly different for any combination of treatment (E8, E6, or BA) or seeding method (colony, single cell; Figure 1E). The percentage of $SOX2^+$ cells, which is indicative of both pluripotent and neuroectodermal cells, was significantly higher in SCS E6 cultures compared with SCS E8 and BA (Figures 1D and 1E). Virtually no expression of SOX2 in SCS BA was observed, suggesting a loss of pluripotency and lack of neuroectoderm differentiation. Expression of Brachyury T (TBXT), a marker of primitive streak and mesendoderm differentiation, was significantly higher in SCS BA cultures compared with SCS E8 and E6 (Figures 1F and 1E). TBXT expression in E8 and E6 cultures (both colony and SCS) was nearly zero, indicating that spontaneous mesendoderm differentiation was not observed within this time frame. Quantification of cell density based on high-content imaging demonstrated no significant differences between seeding method or medium (E8, E6, or BA) after 48 h, indicating that overall cell yield was not affected by SCS.

Protein expression data were corroborated by population-level qPCR analysis (Figure 1G). *POU5F1* (*OCT4*) expression was largely unchanged among all treatments, with significant differences observed only between E6 (SCS and colony) and colony BA. Expression of *SOX2* transcripts was significantly higher in SCS E6 than all other treatments, in agreement with observed protein expression patterns. The expression of early mesoderm and endoderm markers including TBXT, *MIXL1*, *EOMES*, and *GSC* were also assessed by qPCR. With the exception of *GSC*, which was not significantly upregulated compared with colony BA, all of these markers showed higher expression levels in SCS BA compared with all other treatments. Robust induction of mesendoderm genes was also observed in H1 and H7 hESCs following SCS BA treatment (Figure S1C), as was the expression of TBXT and loss of SOX2 proteins (Figure S1D). Collectively, these data demonstrate that SCS of hPSCs improves the uniformity of spatial dispersion and enhances directed mesendoderm differentiation compared with colony seeding.

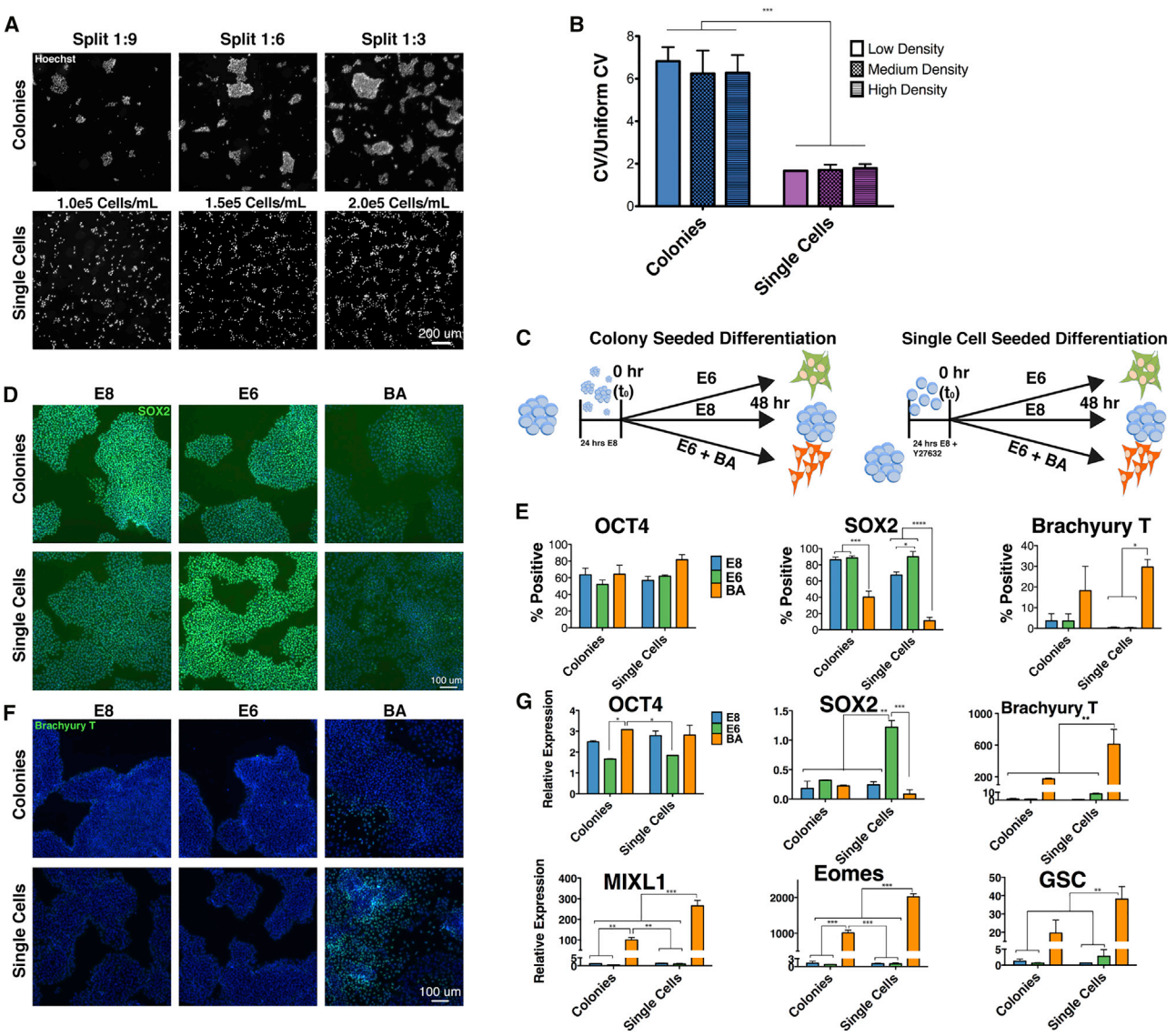

Figure 1. Single-Cell Seeding and BMP4 and Activin A Treatment Enhance Mesendoderm Differentiation

(A) Colony or single-cell seeded (SCS) H9 ESCs were stained with Hoechst and imaged to quantify the spatial positioning of each cell. Scale bar, 200 μm.

(B) The spatial uniformity of cells imaged in (A) was assessed by the coefficient of variation (CV) in the number of cells in 345- × 345-μm grids.

(C) Schematic depiction of colony and SCS differentiation protocol in E8 (blue), E6 (green), or BA (orange) media.

(D) SOX2 staining after 48 h of differentiation in E8, E6, or BA conditions following colony or SCS. Scale bar, 100 μm.

(E) Quantification of immunofluorescent staining for OCT4, SOX2, and TBXT after 48 h via high-content imaging. See also Figure S1D.

(F) Immunofluorescent staining of TBXT after 48 h of differentiation. Scale bar, 100 μm.

(G) Quantification of pluripotency (*OCT4, SOX2*) and mesendoderm (*TBXT, MIXL1, EOMES, GSC*) gene expression by qPCR analysis. See also Figure S1C.

Errors bars represent SEM, n = 3 independent experiments, *p < 0.05, **p < 0.01, ***p < 0.001, ****p < 0.0001 for (B), (E), and (G).

BA Treatment Induces Mesendoderm Gene Expression Signatures

After ascertaining that SCS could induce robust differentiation of hPSCs, we next sought to assess global transcriptomic changes in cells treated with E8, E6, and BA by RNA sequencing (RNA-seq). A common undifferentiated sample (i.e., t0) as well as 48-h E8, E6, and BA samples were sequenced, along with a 24-h BA time point. E8 and

E6 samples clustered separately from the 24- and 48-h BA samples, as indicated by hierarchical clustering (Figure 2A). Mesendoderm genes were found to be strongly upregulated in the 24- and 48-h time points following BA treatment, including *TBXT*, *EOMES*, *GATA5*, and *MIXL1* (Figure 2A, red boxes), while neuroectoderm-associated genes were strongly downregulated, including *HES3*, *HTR1A*, *EMX1*, and *LRAT* (Figure 2A, blue box). Gene ontology (GO) terms associated with ion channel regulation and nervous system development were enriched in the E6 samples, suggesting that E6 medium is permissive of a neuroectoderm fate specification. In contrast, terms associated with general differentiation (embryo development/morphogenesis, tissue/organ morphogenesis) as well as mesoderm-specific differentiation (circulatory/cardiovascular/blood vessel development, heart development) were strongly enriched at both 24 and 48 h in the BA-treated cells. In addition, gene set enrichment analysis (GSEA) of the 48-h BA samples demonstrated that mesendoderm, lateral plate mesoderm, and pre-cartilage condensation gene sets were significantly enriched ($p < 0.0041$), while the Neural Ectoderm gene set was not enriched ($p = 0.164$) (Figure 2C). Together, GSEA and GO analysis demonstrate that SCS BA treatment induced a gene expression signature indicative of mesendoderm and mesoderm differentiation, while E6 treatment induced early neuroectoderm specification.

Dynamic Transcriptional Networks Regulate Mesendoderm Specification

While transcriptomic analysis after 1 and 2 days of differentiation identified distinct gene expression profiles in the three treatment groups, we hypothesized that a higher-resolution kinetic analysis would reveal deeper insight into mesendoderm commitment. At 6-h intervals, samples were collected in the three differentiation conditions for the duration of the 48-h time course, and RNA-seq was performed. Whereas E8 and E6 samples clustered randomly, the BA samples all clustered sequentially from 6 to 48 h, as indicated by hierarchical clustering (Figure 3A; full fold change data in Table S4). This observation is further supported by principal-component analysis, with random grouping of E6 and E8 time points contrasting an ordered trajectory of BA samples in the first two principal component dimensions (Figure 3B).

To functionally categorize dynamic gene expression events that regulate mesendoderm differentiation, differentially expressed genes were clustered into discreet paths based on similarity of expression kinetics (Figure 3C). The unique gene sets comprising each path were then queried individually for enriched GO terms. Genes that were upregulated early but quickly plateaued in expression level (path1) enriched GO terms related to response to growth factor stimulus, such as regulation of SMAD phosphorylation and BMP signaling (full GO analysis can be found in Table S1). Similarly, a query of all genes upregulated in BA after 12 h also enriched terms related to signaling pathways (Figure 3D). Genes that were upregulated at early time points and continued to be strongly upregulated throughout differentiation (path 2) enriched GO terms related to general differentiation events, such as embryonic morphogenesis, but also more specific terms such as heart development. Genes with expression trajectories that increased at later stages of differentiation (path 3) enriched terms related to specific differentiation events, such as blood vessel development, skeletal system development, and organ morphogenesis. Collectively, analysis of these upward trajectories indicates that transcriptional response to SCS BA induction occurs in waves, whereby cells initially respond to changes in the signaling environment, followed by general differentiation and morphogenesis, and finally specific differentiation events. Genes clustered in paths with a downward trajectory (paths 4, 5, and 6) enriched terms related to nervous system and neural development and differentiation. This enrichment was similar to that observed with query of genes upregulated at 48 h in E6 (Figure 2B) as well as genes downregulated at 48 h in BA (Figure 3D). Broader investigation of all significantly enriched biological process GO terms for genes upregulated at 48 h following BA treatment revealed many terms related to specific mesoderm and endoderm cell lineages, including heart development, mesoderm development, blood vessel development, regulation of muscle development, mesenchymal cell differentiation, and endoderm development (Figure 3E). These data indicate that after 48 h of BA treatment, cells may have the potential to be further instructed to differentiate to a variety of mesoderm cell types, thereby making the SCS BA protocol amenable to a breadth of tissue engineering applications.

Heterogeneous Populations of Mesoderm and Endoderm Cells Are Produced from Initial Single-Cell BA Treatment

To address the potential for population heterogeneity contributing to transcriptomic analysis, differentiation at the single-cell level was assessed via single-cell qPCR using a 96-gene panel of pluripotency and differentiation markers on the Fluidigm platform (Figure 4A). Similar to population-level RNA-seq data, cells grown in E8, E6, or BA conditions for 48 h clustered into distinct groups, as revealed by hierarchical clustering analysis (Figure 4B). Similarly, distinct populations of cells between the three treatment groups were observed on a t-distributed stochastic neighbor embedding (t-SNE) plot (Figure 4C), suggesting that distinct transcriptional profiles exist for each treatment at the single-cell level. The cluster of genes that distinguished BA cells from E6 and E8 (red

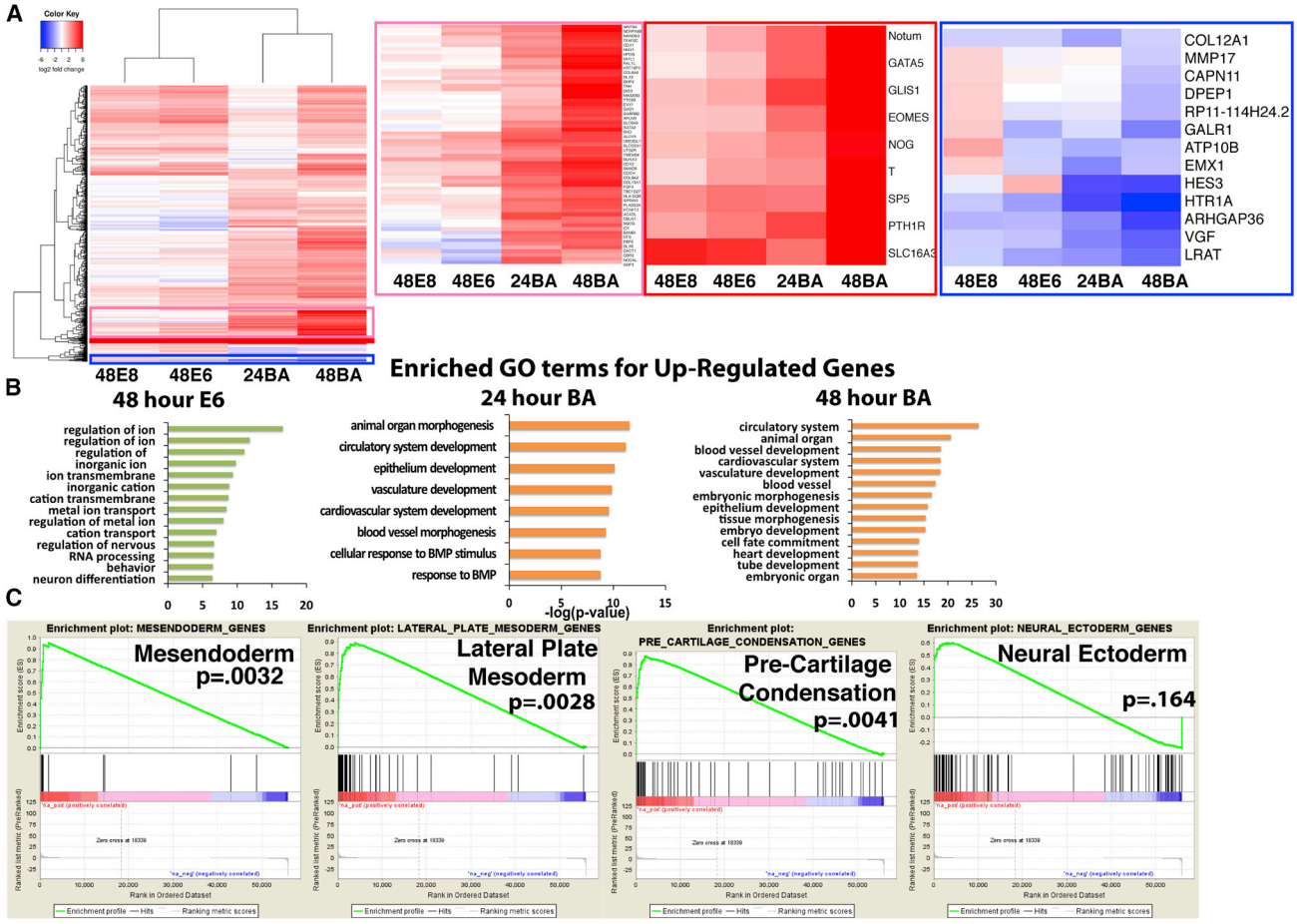

Figure 2. Transcriptomic Analysis of E8, E6, and BA Treatments by RNA-Seq

(A) Heatmap of differentially expressed genes between 48-h E8, 48-h E6, and 24- and 48-h BA samples. Heatmaps of selected clusters of genes upregulated in BA (pink box), strongly upregulated in BA (red box) or downregulated in BA samples (blue box) are enlarged.

(B) Enriched GO terms for genes upregulated in 48-h E6, 24-h BA, and 48-h BA samples.

(C) Gene set enrichment analysis (GSEA) of 48-h BA samples for mesendoderm, lateral plate mesoderm, cartilage condensation, and neural ectoderm gene sets.

box), including *TBXT*, *APLNR*, *GATA6*, *PDGFRA*, *CER1*, *GSC*, and *EOMES*, was enriched for tissues associated with mesoderm and endoderm lineages (Figure 4D). To assess heterogeneity within the 48-h BA population, co-expression of different combinations of genes within this cluster was visualized (Figure S2). Of 36 BA cells that expressed *PDGFRA*, *TBXT*, *EOMES*, or *GSC*, 6 cells expressed all 4 of these genes at high levels, 11 cells expressed 3 of the 4 genes, 10 expressed 2 genes, whereas only 8 cells expressed only one gene. Co-expression of endoderm genes *SOX17* and *GATA6* with mesoderm marker *PDGFRA* was assessed, revealing that 20 of 22 *PDGFRA*$^{+}$ cells also expressed *SOX17*, *GATA6*, or both *SOX17* and *GATA6*, suggesting that cells express both mesoderm and endoderm markers at this stage. Co-expression of *SOX17* and *GATA6* with additional mesendoderm genes, including *TBXT*, *EOMES*, and *GSC* further supports the mixed expression profile of these cells. Collectively, these data demonstrate that while heterogeneity in gene expression signature exists at 48 h, a significant fraction of cells co-expressed markers of primitive streak and mesoderm and endoderm lineages.

To assess the differentiation potential of cells pre-differentiated in E8, E6, or BA, pretreated cells were allowed to differentiate in basal conditions (E6 or E6 supplemented with B27) for a total of 2 weeks (48 h + 12 additional days). Single-cell analysis of differentiation at the 2-week time point was assessed using the same 96-gene panel as the 48-h time point. Similar to the 48-h time point, BA-treated cells clustered separately from E6 and E8 cells by both hierarchical clustering (Figure 4E) and t-SNE (Figure 4F). Interestingly, E6 and E8 samples clustered among

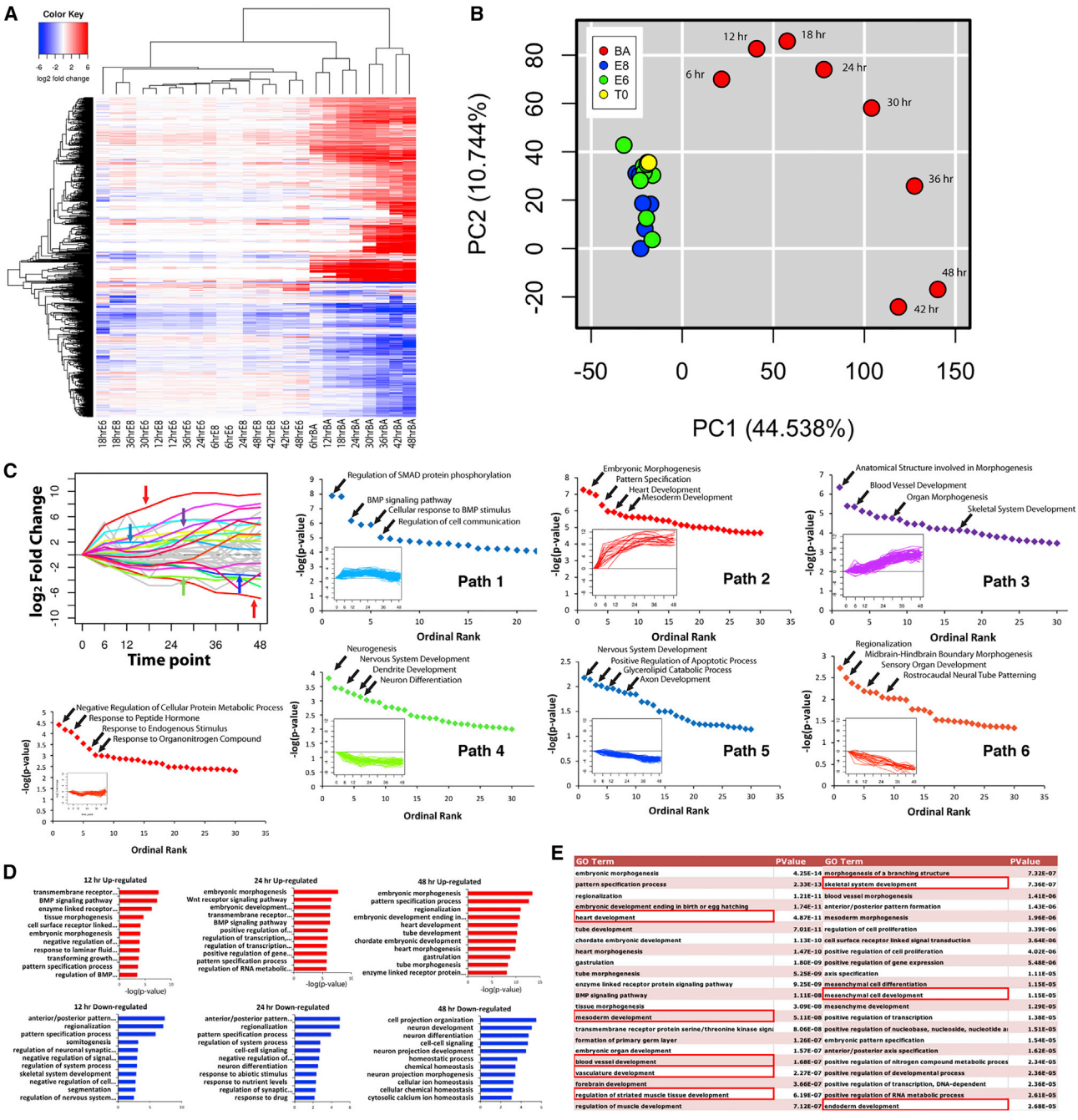

E

GO Term	PValue	GO Term	PValue
embryonic morphogenesis	4.25E-14	morphogenesis of a branching structure	7.32E-07
pattern specification process	2.33E-13	skeletal system development	7.36E-07
regionalization	1.21E-11	blood vessel morphogenesis	1.41E-06
embryonic development ending in birth or egg hatching	1.74E-11	anterior/posterior pattern formation	1.43E-06
heart development	4.87E-11	mesoderm morphogenesis	1.96E-06
tube development	7.01E-11	regulation of cell proliferation	3.39E-06
chordate embryonic development	1.13E-10	cell surface receptor linked signal transduction	3.64E-06
heart morphogenesis	1.47E-10	positive regulation of cell proliferation	4.02E-06
gastrulation	1.80E-09	positive regulation of gene expression	5.48E-06
tube morphogenesis	5.25E-09	axis specification	1.11E-05
enzyme linked receptor protein signaling pathway	9.25E-09	mesenchymal cell differentiation	1.15E-05
BMP signaling pathway	1.11E-08	mesenchymal cell development	1.15E-05
tissue morphogenesis	3.09E-08	mesenchyme development	1.29E-05
mesoderm development	5.11E-08	positive regulation of transcription	1.38E-05
transmembrane receptor protein serine/threonine kinase signi	8.06E-08	positive regulation of nucleobase, nucleoside, nucleotide a	1.51E-05
formation of primary germ layer	1.26E-07	embryonic pattern specification	1.54E-05
embryonic organ development	1.57E-07	anterior/posterior axis specification	1.62E-05
blood vessel development	1.68E-07	positive regulation of nitrogen compound metabolic proces	2.34E-05
vasculature development	2.27E-07	positive regulation of developmental process	2.36E-05
forebrain development	3.66E-07	positive regulation of transcription, DNA-dependent	2.36E-05
regulation of striated muscle tissue development	6.19E-07	positive regulation of RNA metabolic process	2.61E-05
regulation of muscle development	7.12E-07	endoderm development	2.68E-05

Figure 3. Time Course Transcriptomic Analysis for E8, E6, and BA Samples at 6-h Intervals for 48 h

(A) Heatmap of differentially expressed genes, with hierarchical clustering sequentially grouping each BA time point.

(B) Principal component analysis showing the E8 and E6 samples clustering together, while the BA samples display an ordered trajectory.

(C) Genes differentially expressed in BA samples were clustered into paths based on similarity of temporal expression. Genes comprising each path were analyzed for enriched GO terms for upward trajectories (top row), downward trajectories (bottom row), and a trajectory with upward and downward components (bottom left panel).

(D) Enriched GO terms for genes upregulated (top row, red bars) and downregulated (bottom row, blue bars) in BA samples at 12-, 24-, and 48-h time points.

(E) List of enriched GO terms for genes upregulated at 48 h in BA samples, with terms related to mesoderm and endoderm differentiation highlighted.

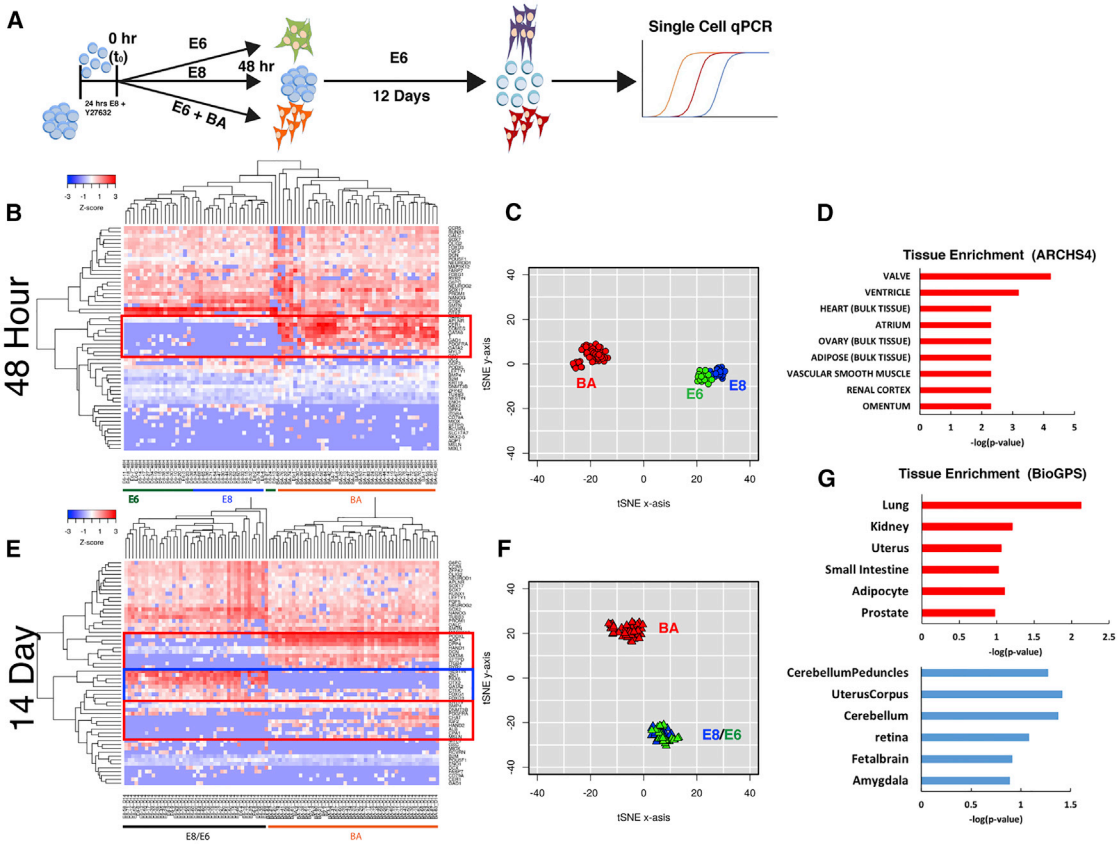

Figure 4. Single-Cell Gene Expression Analysis

(A) Schematic depiction of single-cell gene expression analysis at 48-h and 14-day time points.

(B) Heatmap of expression levels of the panel of genes in individual cells after 48 h in E8, E6, or BA. Genes upregulated in BA cells are highlighted (red box).

(C) t-SNE plot of individual cells, with E8 cells in blue, E6 in green, and BA in red.

(D) Genes in the red box were analyzed for tissue enrichment using EnrichR.

(E) Heatmap of expression levels of the panel of genes in individual cells after 14 days. Genes upregulated in BA cells are highlighted in red boxes and genes upregulated in E8 and E6 cells are highlighted in the blue box.

(F) t-SNE plot of individual after 14 days (E8 blue, E6 green, and BA red).

(G) Genes upregulated in BA cells (red boxes in E) were analyzed for tissue enrichment in EnrichR (top, red bars), as were genes upregulated in E8/E6 cells (blue box in E), bottom graph with blue bars.

See also Figure S2.

each other, suggesting that pre-differentiation in E6 is not sufficient to alter the long-term differentiation trajectory of cells in basal conditions. A number of genes were highly expressed in the BA-treated population and not expressed in the E6/E8 populations, including *HAND1*, *DCN*, *GATA6*, *AQP1*, *ITGB4*, and *DPP4* (Figure 4E, red boxes), suggestive of mesoderm and endoderm cell lineages. Tissue enrichment analysis for the genes upregulated in 14-day BA cells identified mesoderm and endoderm-derived tissues as most significantly enriched, including lung, kidney, and uterus (Figure 4G, top). Genes that were highly expressed in E6/E8 samples but not BA samples included *PAX6*, *OTX2*, *ZIC1*, *NES*, *GATA2*, *TUBB3*, *SOX2*, and *OLIG2* (Figure 4E, blue box), strongly suggestive of a neuroectoderm phenotype. Enriched tissue analysis for these genes upregulated in E6/E8 cells identified largely brain- and ectoderm-related terms (Figure 4G, bottom). The single-cell gene expression observed is consistent with the dense neurite projections and connectivity that was observed in the E6 and E8 samples, but not BA, after 14 days and indicates that pre-differentiation in E6/E8 allows cells to follow a default trajectory to a neuroectoderm fate. Thus, pre-differentiation in BA is permissive to downstream differentiation to both mesoderm and endoderm lineages but diminishes ectoderm potential.

Pre-differentiation in BA Enhances Chondrocyte Progenitor and Endothelial Progenitor Commitment and Supports Definitive Endoderm Induction

Population transcriptomic analysis and single-cell qPCR data demonstrated that SCS BA differentiation produced a cell population with a gene expression profile indicative of mesoderm and endoderm-derived cells, and previous studies have utilized an adapted version of our protocol to produce skeletal muscle progenitor cells (Shelton et al., 2014, 2016). Therefore, we hypothesized that cells treated for 48 h in BA could be subsequently specified into mature cell types using existing protocols with enhanced efficiency. The cartilage condensation gene set was shown to be significantly enriched after 48-h BA treatment (Figure 2C), and GO terms related to blood vessel and vasculature development were also found to be significantly enriched following BA treatment (Figures 3C and 3E). Based on this transcriptomic analysis, existing protocols for chondrogenesis and endothelial progenitor cell (EPC) differentiation were targeted to be modified to include SCS BA pretreatment. For chondrocyte induction, micromass culture (Toh et al., 2009) was adapted to include the 48-h pretreatment protocol in place of embryoid body (EB) formation for H9 hESCs as well as two iPSC lines derived in our lab, as depicted in Figure 5A. Sulfated glycosaminoglycan (s-GAG) and collagen levels (hydroxy-proline) were quantified after 7 days of micromass culture, and both s-GAG levels and hydroxy-proline expression were significantly higher following BA pretreatment compared with E8 and E6 (Figure 5B). Proteoglycan production, visualized via Alcian blue staining, was also notably more pronounced in BA-pretreated cells than either E8 or E6 treatments (Figure 5C). The increase in glycosaminoglycan and collagen production was consistently observed for H9 hESCs and two iPSC lines, demonstrating that SCS BA is amenable to a chondrogenic protocol, and that it is efficacious in robustly enhancing the differentiation of three independent PSC lines.

An EPC differentiation protocol (Tatsumi et al., 2011) was similarly modified to include E8, E6, or BA pretreatment in previously derived iPSCs (Chang et al., 2013). To assess EPC differentiation, expression of a number of surface markers was quantified using flow cytometry (Figure 5D). After 6 days of differentiation, BA-pretreated cells contained a higher proportion of CD31-, CD144-, and VEGFR-2-positive cells than E6 or E8, indicating higher percentages of endothelial cell differentiation. This again demonstrates that the BA population at 48 h can be efficiently directed to different cell types given the proper instructive cues.

Although chondrocyte progenitor and EPC differentiation demonstrate the mesodermal potential of SCS BA-treated cells, we also sought to assay the definitive endodermal (DE) capacity of the SCS BA treatment. Cells initially subjected to 48-h BA treatment (or E8/E6 controls) were subsequently differentiated using E6 medium supplemented with high Activin A (100 ng/mL) with or without the BMP inhibitor LDN193189 (250 nM) (Figure 5E), based on a previously described protocol (Loh et al., 2014). These experiments suggested that BA concentrations of 10 and 60 ng/mL, respectively, more efficiently induced DE differentiation than 40/40 ng/mL; therefore, 10/60 SCS BA conditions were used for DE induction. After 96 h of DE differentiation, H9 hESCs treated with Activin A alone or Activin A + LDN were >50% SOX17$^+$, indicating a high proportion of DE cells (Figures 5F and 5G). FOXA2 staining further confirmed the DE phenotype of these cells, as did expression of *SOX17*, *FOXA2*, and *GATA6* genes (Figure 5H). Expression of the visceral endoderm marker *AFP* was not significantly enhanced following BA pretreatment. *MIXL1* expression in BA-treated cells indicated that a subpopulation of mesoderm cells remains following the DE induction protocol. Similar trends in DE differentiation were observed in H1 and H7 hESCs (Figure S3). Thus, the SCS BA protocol enhances mesodermal differentiation but is also permissive of definitive endoderm commitment; however, higher Activin A and lower BMP4 concentrations support more robust DE induction.

BA Treatment Suppresses Spontaneous and Directed Neuroectoderm Differentiation

Enriched GO terms for genes downregulated upon BA treatment were frequently associated with neural differentiation (Figure 3D), and Neural Ectoderm genes were negative for enrichment in GSEA (Figure 2C). We therefore hypothesized that, after pretreatment in BA for 48 h, cells would be refractory to neural induction. To test this hypothesis, cells treated with E8, E6, or BA were subjected to a common neural differentiation protocol that utilizes dual SMAD inhibition via treatment with LDN193189 and SB431542, inhibitors of BMP and TGF-β, respectively (Chambers et al., 2009). After 48 h of pre-differentiation, medium was replaced with either E6 alone, or E6 containing LDN and SB and cultured for a further 3 days (Figure 6A). At the 48-h time point, cells treated with E8 or E6 expressed SOX2 (80% and 88%, respectively), while BA cells showed virtually no expression (2.5% SOX2$^+$; Figures 6B and 6C). Cells treated with E8 expressed high levels of *OCT4*, *NANOG*, and *SOX2* transcripts at the 48-h time point (Figure 6D), confirming that these cells remain in a pluripotent state, whereas the E6 treatment resulted in high expression of *SOX2* and *OTX2* with reduced *OCT4* and *NANOG*, suggesting a loss of pluripotency and early neuroectoderm commitment (Figure 6D). Mesendoderm commitment of BA-treated cells was confirmed, as TBXT was expressed exclusively in BA-treated cells (Figure 6B), consistent with

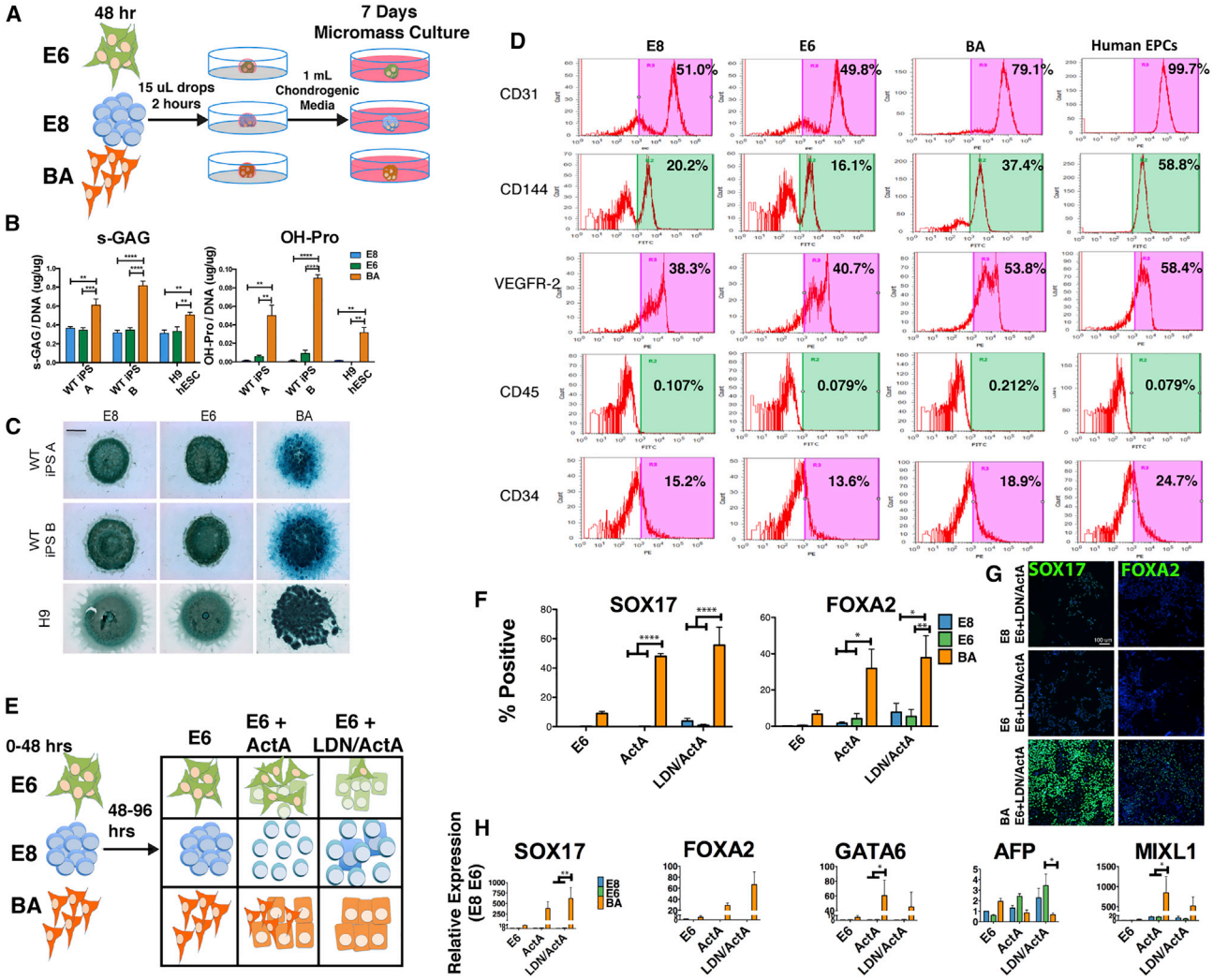

Figure 5. Chondrocyte, Endothelial Progenitor Cell, and Definitive Endoderm Differentiation Following BA Pretreatment

(A) Schematic depicting the micromass culture protocol utilizing E8 (blue), E6 (green), or BA (orange) pretreatment.

(B) Sulfated glycosaminoglycan (left) and hydroxy-proline (right) levels were elevated in BA-treated cells compared with both E6 and E8 in two iPSC lines and H9 hESCs after 7 days of micromass culture.

(C) Alcian blue staining for proteoglycan production after 7 days of micromass culture. Scale bar, 2 mm.

(D) Flow cytometry analysis of cell surface marker expression after integration of E8-, E6-, or BA-pretreated cells into an EPC differentiation protocol. Isotype immunoglobulin antibody was used as a negative control.

(E) Schematic representation of definitive endoderm induction protocol.

(F and G) Quantification (F) of $SOX17^+$ and $FOXA2^+$ cell populations based on immunofluorescent staining in (G). Scale bar, 100 μm.

(H) Gene expression analysis of DE genes *SOX17*, *FOXA2*, *GATA6*, visceral endoderm gene *AFP*, and mesendoderm/mesoderm gene *MIXL1*, following the 96-h DE induction protocol.

Errors bars represent SEM, n = 3 independent experiments, *p < 0.05, **p < 0.01, ***p < 0.001, ****p < 0.0001 for (B), (F), and (H). See also Figure S3.

Figure 1E. In addition, the loss of *NANOG* and *SOX2* expression along with high expression levels of *OCT4* and *MIXL1* further confirm mesendoderm commitment of BA cells at 48 h (Figure 6D). Following 5 days of differentiation in both E6 and dual inhibition, pluripotency was lost in all conditions, because a total abrogation of *OCT4* and *NANOG* expression was observed (Figure 6D). High levels of SOX2 expression (both protein and transcript) in E8 and E6 samples was observed, whereas significantly lower SOX2 expression was observed for BA samples in both types of media (Figures 6B and 6D). Similarly, the intermediate filament protein Nestin was expressed significantly

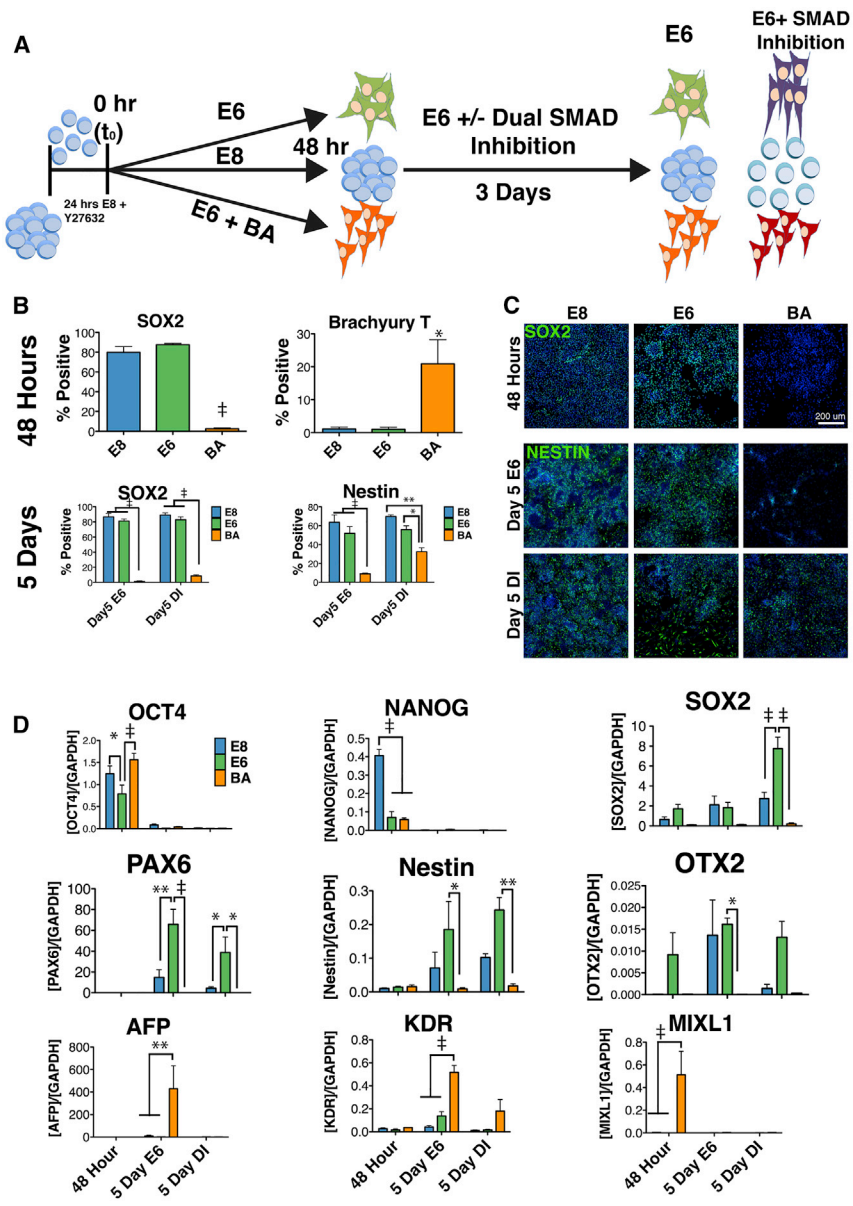

Figure 6. Pretreatment with BA for 48 h Repressed Neuroectoderm Potential

(A) Schematic depicting the neuro-induction protocol using E8-, E6-, or BA-pretreated cells as the input population.

(B and C) Quantification (B) and representative images (C) of immunofluorescent staining for SOX2 and TBXT after 48 h, and SOX2 and Nestin after 5 days.

(D) Gene expression analysis after 48 h, 5 days in E6, and 5 days in dual SMAD inhibition (DI) medium for E8-, E6-, and BA-pretreated cells. Pluripotency (*OCT4*, *NANOG*, *SOX2*), neuroectodoerm (*SOX2*, *PAX6*, *NES*, *OTX2*), and mesoderm/endoderm (*AFP*, *KDR*, *MIXL1*) genes were assessed.

Error bars represent SEM, n = 3 independent experiments, *p < 0.05, **p < 0.01, ‡ = p < 0.001 for (B) and (D). Scale bar, 200 μm.

higher in E8- and E6-pretreated cells in both E6 and dual inhibition media. Spontaneous neuroinduction (E6) was nearly absent in BA-pretreated cells (1% SOX2$^+$, 9% Nestin$^+$), while significantly lower directed neuroinduction (dual inhibition) was observed compared with E8 or E6 pretreatment. Expression of neural differentiation genes, including *SOX2*, *PAX6*, *OTX2*, and *NES* was extremely low for BA pretreatment in either E6 or dual inhibition media. Finally, BA-pretreated cells allowed to spontaneously differentiate in E6 expressed high levels of *AFP* and *KDR*, demonstrating differentiation of mesendoderm-derived lineages.

Teratomas Preferentially Form Mesoderm and Endoderm Lineages Following BA Treatment

Cells subjected to SCS BA treatment demonstrated efficient induction of mesendoderm after 48 h, enhanced efficiency of differentiation of mesoderm lineages, and reduced capacity for neuroectoderm specification under defined conditions *in vitro*. Thus, we hypothesized that, in an *in vivo* environment that is permissive to the formation of all three germ lineages (i.e., teratoma formation), BA-pretreated cells would preferentially differentiate to mesoderm and endoderm lineages and reduced ectoderm lineages compared with E8 and E6 treatment.

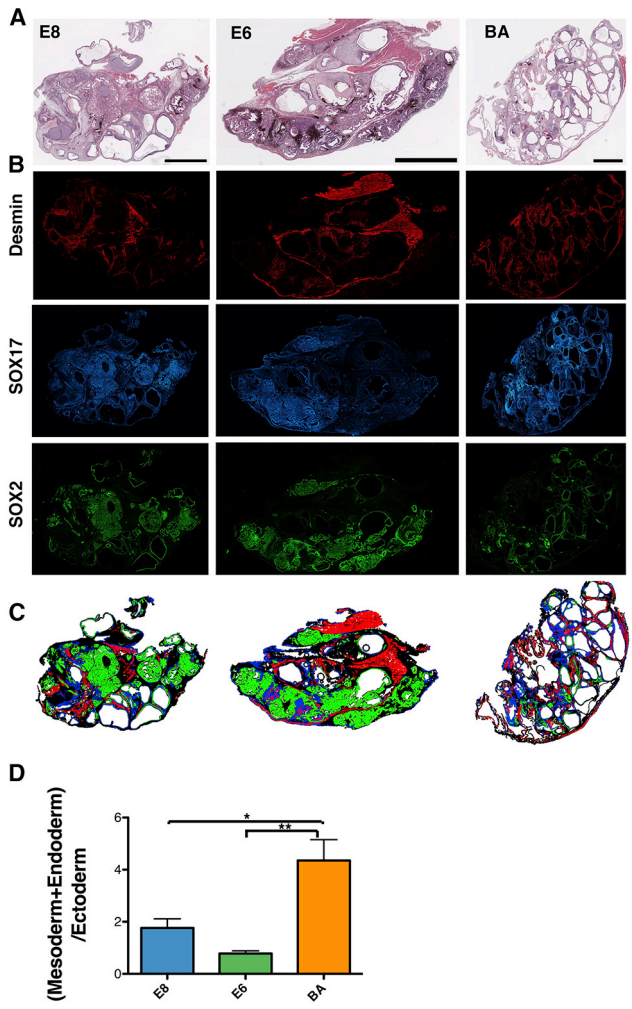

Figure 7. Analysis and Quantification of Teratomas Formed from E8-, E6-, and BA-Treated Cells

(A) H&E staining of teratomas derived from E8-, E6-, or BA-pretreated cells.

(B) Immunofluorescent staining of teratoma sections for Desmin (mesoderm), SOX17 (endoderm), and SOX2 (ectoderm).

(C) Images from adjacent sections in (B) were merged and the percentage of each germ layer in each teratoma section was assessed.

(D) Quantification of the combined mesoderm and endoderm to ectoderm area ratio for teratomas formed from E8-, E6-, and BA-treated cells. For each teratoma, 3 regions at least 150 μm apart were analyzed, and 4 × 10^6, 5 × 10^8, and 6 BA teratomas were used.

Scale bars, 2 mm. Error bars represent SEM; *$p < 0.05$, **$p < 0.005$.

To test this hypothesis, cells pretreated with E8, E6, or BA for 48 h were injected into the hindlimbs of *NOD/SCID* mice to induce teratoma formation. After 9–18 weeks of teratoma growth, tumors were excised, fixed, sectioned, and stained with H&E to identify tissue structures, including cartilage and pigmented epithelium (Figure 7A). The formation of primary germ layers was further assessed via immunofluorescent staining for SOX2 (ectoderm), SOX17 (endoderm), and Desmin (mesoderm) (Figures 7B and 7C). The ratio of mesoderm and endoderm lineages to ectoderm was calculated for the entire teratoma area of three sections from at least four teratomas for each treatment (Figure 7D). Cells pretreated with BA formed teratomas with the highest mesoderm + endoderm to ectoderm ratio, while E6 treatment produced the lowest such ratio ($p < 0.05 \times 10^6$ versus BA). Treatment with E8 resulted in teratomas with a ratio of ~2 (1.8 ± 0.3), indicating an equal proportion of mesendoderm and ectoderm lineages. Ratios of 4.4 ± 0.8 for BA and 0.8 ± 0.1 for E6 indicate strong bias for mesendoderm and ectoderm differentiation, respectively. Thus, the 48-h pre-differentiation in BA specifies cells on a differentiation trajectory which, in an *in vivo* environment permissive to formation of germ layers in roughly equal proportions, results in commitment to mesendoderm lineages at the expense of ectoderm formation.

DISCUSSION

In this work we describe a simple, robust method for reproducible mesendoderm induction of human PSCs. Transcriptomic data indicated that the cell population produced at 48 h would be amenable to directed differentiation of cell types including chondrocytes and EPCs, which was confirmed experimentally. We further demonstrated that the levels of BA in the SCS BA protocol could be modified to support integration into a DE differentiation protocol, highlighting the adaptability of the technique.

We demonstrate that SCS of PSCs results in quantifiably more homogeneous spatial cellular distribution compared with colony-based seeding. Colony-based seeding strategies can be problematic for reproducibility for a number of reasons. The size and distribution of seeded colonies is a function of the initial colony size, the degree to which colonies are broken up, and the split ratio. Protocols often note the degree of confluency to target before splitting or starting differentiation, which is an approximate and subjective metric dependent on both initial colony seeding density and colony size. By reducing colonies to a single-cell suspension before seeding and plating a fixed cell density, we avoided the common issues associated with colony seeding and significantly improved the uniformity and reproducibility of spatial distributions. Furthermore, the parameters we use to define our method are quantitative

and objective, allowing others to easily replicate the protocol.

Previous work has demonstrated that numerous combinations of growth factors, small molecules, and cytokines can be used to induce mesendoderm differentiation from hPSCs. For example, Touboul et al. (2010) have used a cocktail consisting of Activin A, FGF2, BMP4, and Ly93092 (termed AFBLy) to induce DE lineages, and variations upon this combination to induce other lineages (e.g., FLyA for endoderm, FLyB for mesoderm; Bernardo et al., 2011). Loh et al. (2014) elucidated the signaling components necessary to induce primitive streak and DE from hPSCs, demonstrating that FGF, BMP, and WNT signaling are required for primitive streak formation. While the studies mentioned above have all utilized monolayer culture, EB-based protocols are also commonly used. EB-based methods for mesoderm induction (cardiac myocytes or chondrocytes) utilize 1 day of BMP4 treatment followed by an additional 2 days of BA and FGF2 treatment (Craft et al., 2015; Kattman et al., 2011; Lee et al., 2017; Protze et al., 2016). The specific concentration of growth factors depends on the targeted cell lineage and the cell line used for induction. Definitive endoderm-derived lineages, including pancreatic cells and hepatocytes, can also be produced from EBs using a similar growth factor cocktail, albeit with higher levels of Activin A (Holtzinger et al., 2015; Nostro et al., 2011).

Our mesendoderm induction protocol shares a number of similarities with these existing methods with notable exceptions. Our findings suggest that endogenous levels of WNT and FGF signaling—or perhaps pathway crosstalk—are sufficient for mesendoderm induction in the presence of BA, such that addition of WNT agonists and FGF2 is not required. Interestingly, the specific concentrations of growth factors used varies greatly between protocols. For example, Teo et al. (2012) reported DE induction with both BA concentrations of 50 ng/mL, whereas many other DE protocols use Activin A levels as high as 100 ng/mL (Bernardo et al., 2011; Brown et al., 2011; Holtzinger et al., 2015; Nostro et al., 2015). For induction of mesoderm, much lower levels of both Activin A and BMP4 have been utilized (1–10 ng/mL, depending on the cell line and target lineage) (Craft et al., 2015; Kattman et al., 2011; Lee et al., 2017; Protze et al., 2016). In the presence of FGF2 and phosphatidylinositol 3-kinase inhibitor (Ly294002), Activin A alone (100 ng/mL) was sufficient to induce DE induction, even in the presence of BMP inhibitor Noggin, while BMP4 alone (10 ng/mL) was able to induce mesoderm in the presence of Activin A inhibitor SB431542 (Bernardo et al., 2011). We demonstrate that 40 ng/mL of both Activin A and BMP4 is ideal for mesendoderm induction in our SCS culture method. However, while 40/40 was efficient in inducing mesoderm differentiation, reduction of BMP4 to 10 ng/mL and increase of Activin A to 60 ng/mL was required for high levels of DE differentiation, in agreement with previous findings that gradients of BA specify sub-populations of primitive streak (Kattman et al., 2011). In addition, the conditions under which hPSCs are maintained for self-renewal may contribute to how cells respond to differentiation conditions, as a variety of approaches exist for maintenance, including use of feeder cells (MEFs) and Knock Out Serum Replacement (KOSR), MEF-conditioned media, mTESR, and E8, as well as a variety of tissue culture coatings including Matrigel and Vitronectin. Transcriptomic studies indicate that variation between pluripotent cell lines is extensive (Adewumi et al., 2007) and that much of the variance can be attributed to the lab in which the cells are cultured (Chin et al., 2009; Newman and Cooper, 2010), suggesting that PSCs are exquisitely sensitive to culture conditions.

We describe a defined differentiation system for the robust induction of a mesendoderm population. Although many studies focus on identifying conditions to direct differentiation to one specific cell type, we developed a system amenable to the derivation multiple lineages. Furthermore, the BA concentrations in our SCS protocol can be optimized to be integrated into a variety mesoderm- and endoderm-derived cell differentiation protocols.

EXPERIMENTAL PROCEDURES

Cell Lines and Cell Culture

A total of six different human PSC lines were used in this study to test the robustness of the protocols, including H9, H1, and H7 hESCs, and wild-type iPSCs derived from fibroblasts obtained from the Coriell Institute Biobank (GM00969) (chondrogenic assays) or from late EPCs (Chang et al., 2013) (EPC differentiation assays). Retroviral reprogramming was performed in defined conditions as described previously (Chang et al., 2013). PSCs were maintained in E8 medium (Chen et al., 2011) on Matrigel (BD Biosciences)-coated 6-well tissue culture plates, as described previously (Chang et al., 2013). Passaging of hPSCs was done using 0.5 mM EDTA solution as a gentle dissociation agent.

Colony and Single-Cell Seeding and Differentiation

For colony seeding spatial analysis and differentiation, cells were passaged as described above with EDTA and split at 1:3, 1:6, or 1:9 ratios. After overnight colony seeding in E8, the medium was replaced with fresh E8, E6, or E6 with 40 ng/mL BA (R&D Systems or Peprotech). To induce mesendoderm differentiation via SCS, hPSCs were treated with 10 μm ROCK inhibitor Y-27632 (Tocris) for at least 1 h before dissociating cells with TrypLE Express (Gibco) for 5–7 min. An equal volume of E8 containing 15% KOSR (Gibco) was added and the cell suspension before trituration with P1000. Cells were pelleted by centrifugation (180 rcf, 5 min), resuspended in fresh E8 containing 10 μm Y-27632, and a sample was taken for cell counting (Cellometer Auto, 2000; Nexcelom Bioscience). Cells

were then resuspended at a density of 1.5 × 10^5 cells/mL and plated into freshly Matrigel-coated 6- or 12-well tissue culture plates. Seeding densities of 1.0 × 10^5 to 2.0 × 10^5 cells/mL were also examined in some experiments. After overnight seeding, E8 medium containing Y-27632 was aspirated and replaced with either fresh E8, E6, or E6 with 40 ng/mL BA, except where different BA concentrations are stated. Cells were allowed to differentiate for 48 h, with medium exchanged after 24 h.

Spatial Analysis

Cells were seeded overnight as colonies or single cells, fixed for 15 min in cold 4% paraformaldehyde (PFA), and washed 3× in PBS. Cell nuclei were staining with Hoechst 33342 (Invitrogen) diluted 1:5,000 in PBS for 10 min. Imaging of fixed and stained cells was performed using the Cellomics ArrayScan VTI (Thermo Fisher Scientific) high-content imaging instrument. For each condition, the entire well was scanned, the spatial coordinates of each cell in the plate were acquired, and analysis was performed as described in Supplemental Experimental Procedures.

RNA-Seq

Extraction of RNA from three biological replicates of time course differentiation in E8, E6, and BA was performed using the Macherey-Nagel Nucleospin kit. Concentration and clean-up of RNA was performed via ethanol/sodium acetate precipitation. Samples were pooled from three biological replicates for full-time course differentiation experiments (replicates were not pooled for t_0, 24-, and 48-h samples) before library construction and sequencing, which were performed at the McGill University and Genome Quebec Innovation Center using the Illumina TruSeq mRNA stranded prep kit, and HiSeq 2000 sequencer with 50- or 75-bp single-end reads. Description of bioinformatics analysis can be found in Supplemental Experimental Procedures.

Single-Cell Gene Expression

Single-cell gene expression analysis was performed using the Fluidigm system. At each time point (48 h and 14 days), cells were dissociated into a single-cell suspension using TrypLE Express (48 h) or Dispase (14 days). Isolation, RNA extraction, and cDNA synthesis were performed using the C1 system and C1 Single-Cell Preamp Integrated Fluidic Circuit (IFC) system according to the manufacturer's instructions. Gene expression analysis of amplified cDNA was performed using TaqMan gene expression assays (Applied Biosystems) in the BioMark HD on 96.96 Dynamic Array IFCs. Probes are listed in Table S2, and description of analysis can be found in Supplemental Experimental Procedures.

Lineage Differentiation and Analysis

Complete description of chondrocyte micromass, EPC, definitive endoderm, and neural differentiation can be found in Supplemental Experimental Procedures.

Quantitative Polymerase Chain Reaction

Gene expression analysis was performed by reverse transcription qPCR using a Roche LightCycler 480. RNA extraction was carried out using the Macherey-Nagel Nucleospin RNA kit, and cDNA synthesis was done using SuperScript II Reverse Transcriptase (Invitrogen) from 1 μg of RNA. qPCR was performed using cDNA diluted 1:100, 10 μM forward and reverse primers, and 1× Roche LightCycler 480 SYBR Green I MasterMix. Primers are listed in Table S3.

Immunostaining

Cells in 6- or 12-well plates were fixed in cold 4% PFA, blocked, and permeabilized in 2% BSA containing 0.01% Triton X-100 for 30 min, and primary antibodies were added overnight at 4°C. Alexa Fluor secondary antibodies diluted 1:200–1:400 were incubated for 1 h at room temperature. Cell nuclei were stained with Hoechst diluted 1:5,000 in PBS for 10 min at room temperature. Imaging was performed using the Cellomics ArrayScan. Primary antibodies and dilutions used are listed in Supplemental Experimental Procedures.

Teratomas

Complete description of teratoma formation and analysis can be found in Supplemental Experimental Procedures.

Statistical Analysis

Statistical significance was determined using one-way or two-way ANOVA with Tukey or Bonferroni post-hoc tests using GraphPad Prism software. Three biological replicates were used, except where indicated otherwise.

ACCESSION NUMBERS

RNA-seq data are available on Gene Expression Omnibus using accession number GEO: GSE129570.

SUPPLEMENTAL INFORMATION

Supplemental Information can be found online at https://doi.org/10.1016/j.stemcr.2019.11.001.

AUTHOR CONTRIBUTIONS

R.L.C. designed and performed experiments, analyzed data, and wrote the manuscript. S.Y.K. performed chondrogenic differentiation and analysis. M.H. and D.J.S. performed EPC differentiation and analysis. C.D. and J.Y.-L. assisted with teratoma processing and analysis. C.C. assisted with single-cell gene expression analysis. R.M.T. and T.J.P. performed bioinformatics analysis. W.L.S. oversaw design and execution of experiments, interpretation of data, and wrote the manuscript.

ACKNOWLEDGMENTS

The authors thank Christopher Porter and Gareth Palidwor for bioinformatics assistance. This work is supported by grants from the Canadian Institutes of Health Research (MOP-89910), Natural Sciences and Engineering Research Council of Canada (RGPIN 293170-11 and 2016-06081). Infrastructure was supported by the Canadian Foundation for Innovation and the Province of Ontario grants to W.L.S. W.L.S. is supported by a Canada Research Chair in Integrative Stem Cell Biology.

Received: March 7, 2019
Revised: November 3, 2019
Accepted: November 5, 2019
Published: December 5, 2019

REFERENCES

Adewumi, O., Aflatoonian, B., Ahrlund-Richter, L., Amit, M., Andrews, P.W., Beighton, G., Bello, P.A., Benvenisty, N., Berry, L.S., Bevan, S., et al. (2007). Characterization of human embryonic stem cell lines by the International Stem Cell Initiative. Nat. Biotechnol. *25*, 803–816.

Bauwens, C.L., Peerani, R., Niebruegge, S., Woodhouse, K.A., Kumacheva, E., Husain, M., and Zandstra, P.W. (2008). Control of human embryonic stem cell colony and aggregate size heterogeneity influences differentiation trajectories. Stem Cells *26*, 2300–2310.

Bernardo, A.S., Faial, T., Gardner, L., Niakan, K.K., Ortmann, D., Senner, C.E., Callery, E.M., Trotter, M.W., Hemberger, M., Smith, J.C., et al. (2011). BRACHYURY and CDX2 mediate BMP-induced differentiation of human and mouse pluripotent stem cells into embryonic and extraembryonic lineages. Cell Stem Cell *9*, 144–155.

Brown, S., Adrian, T.E.O., Pauklin, S., Hannan, N., Cho, C.H.H., Lim, B., Vardy, L., Dunn, N.R., Trotter, M., Pedersen, R., et al. (2011). Activin/nodal signaling controls divergent transcriptional networks in human embryonic stem cells and in endoderm progenitors. Stem Cells *29*, 1176–1185.

Chambers, S.M., Fasano, C.A., Papapetrou, E.P., Tomishima, M., Sadelain, M., and Studer, L. (2009). Highly efficient neural conversion of human ES and iPS cells by dual inhibition of SMAD signaling. Nat. Biotechnol. *27*, 275–280.

Chang, W.Y., Lavoie, J.R., Kwon, S.Y., Chen, Z., Manias, J.L., Behbahani, J., Ling, V., Kandel, R.A., Stewart, D.J., and Stanford, W.L. (2013). Feeder-independent derivation of induced-pluripotent stem cells from peripheral blood endothelial progenitor cells. Stem Cell Res. *10*, 195–202.

Chen, G., Gulbranson, D.R., Hou, Z., Bolin, J.M., Ruotti, V., Probasco, M.D., Smuga-Otto, K., Howden, S.E., Diol, N.R., Propson, N.E., et al. (2011). Chemically defined conditions for human iPSC derivation and culture. Nat. Methods *8*, 424–429.

Chin, M.H., Mason, M.J., Xie, W., Volinia, S., Singer, M., Peterson, C., Ambartsumyan, G., Aimiuwu, O., Richter, L., Zhang, J., et al. (2009). Induced pluripotent stem cells and embryonic stem cells are distinguished by gene expression signatures. Cell Stem Cell *5*, 111–123.

Craft, A.M., Rockel, J.S., Nartiss, Y., Kandel, R.A., Alman, B.A., and Keller, G.M. (2015). Generation of articular chondrocytes from human pluripotent stem cells. Nat. Biotechnol. *33*, 638–645.

Davey, R.E., and Zandstra, P.W. (2006). Spatial organization of embryonic stem cell responsiveness to autocrine Gp130 ligands reveals an autoregulatory stem cell niche. Stem Cells *24*, 2538–2548.

Draper, J.S., Smith, K., Gokhale, P., Moore, H.D., Maltby, E., Johnson, J., Meisner, L., Zwaka, T.P., Thomson, J.A., and Andrews, P.W. (2004). Recurrent gain of chromosomes 17q and 12 in cultured human embryonic stem cells. Nat. Biotechnol. *22*, 53–54.

Evans, M.J., and Kaufman, M.H. (1981). Establishment in culture of pluripotential cells from mouse embryos. Nature *292*, 154–156.

Holtzinger, A., Streeter, P.R., Sarangi, F., Hillborn, S., Niapour, M., Ogawa, S., and Keller, G. (2015). New markers for tracking endoderm induction and hepatocyte differentiation from human pluripotent stem cells. Development *142*, 4253–4265.

Kattman, S.J., Witty, A.D., Gagliardi, M., Dubois, N.C., Niapour, M., Hotta, A., Ellis, J., and Keller, G. (2011). Stage-specific optimization of activin/nodal and BMP signaling promotes cardiac differentiation of mouse and human pluripotent stem cell lines. Cell Stem Cell *8*, 228–240.

Lee, J.H., Protze, S.I., Laksman, Z., Backx, P.H., and Keller, G.M. (2017). Human pluripotent stem cell-derived atrial and ventricular cardiomyocytes develop from distinct mesoderm populations. Cell Stem Cell *21*, 179–194.e4.

Lee, L.H., Peerani, R., Ungrin, M., Joshi, C., Kumacheva, E., and Zandstra, P. (2009). Micropatterning of human embryonic stem cells dissects the mesoderm and endoderm lineages. Stem Cell Res. *2*, 155–162.

Loh, K.M., Ang, L.T., Zhang, J., Kumar, V., Ang, J., Auyeong, J.Q., Lee, K.L., Choo, S.H., Lim, C.Y.Y., Nichane, M., et al. (2014). Efficient endoderm induction from human pluripotent stem cells by logically directing signals controlling lineage bifurcations. Cell Stem Cell *14*, 237–252.

Martin, G.R. (1981). Isolation of a pluripotent cell line from early mouse embryos cultured in medium conditioned by teratocarcinoma stem cells (embryonic stem cells/inner cell masses/differentiation in vitro/embryonal carcinoma cells/growth factors). Proc. Natl. Acad. Sci. U S A *78*, 7634–7638.

Martyn, I., Brivanlou, A.H., and Siggia, E.D. (2019). A wave of WNT signaling balanced by secreted inhibitors controls primitive streak formation in micropattern colonies of human embryonic stem cells. Development *146*, dev172791.

Mitalipova, M.M., Rao, R.R., Hoyer, D.M., Johnson, J.A., Meisner, L.F., Jones, K.L., Dalton, S., and Stice, S.L. (2005). Preserving the genetic integrity of human embryonic stem cells. Nat. Biotechnol. *23*, 19–20.

Nazareth, E.J.P., Ostblom, J.E.E., Lücker, P.B., Shukla, S., Alvarez, M.M., Oh, S.K.W., Yin, T., and Zandstra, P.W. (2013). High-throughput fingerprinting of human pluripotent stem cell fate responses and lineage bias. Nat. Methods *10*, 1225–1231.

Newman, A.M., and Cooper, J.B. (2010). Lab-specific gene expression signatures in pluripotent stem cells. Cell Stem Cell *7*, 258–262.

Nostro, M.C., Sarangi, F., Ogawa, S., Holtzinger, A., Corneo, B., Li, X., Micallef, S.J., Park, I.-H., Basford, C., Wheeler, M.B., et al. (2011). Stage-specific signaling through TGF family members and WNT regulates patterning and pancreatic specification of human pluripotent stem cells. Development *138*, 861–871.

Nostro, M.C., Sarangi, F., Yang, C., Holland, A., Elefanty, A.G., Stanley, E.G., Greiner, D.L., and Keller, G. (2015). Efficient generation of NKX6-1+ pancreatic progenitors from multiple human pluripotent stem cell lines. Stem Cell Reports *4*, 591–604.

Park, I.-H., Arora, N., Huo, H., Maherali, N., Ahfeldt, T., Shimamura, A., Lensch, M.W., Cowan, C., Hochedlinger, K., and Daley,

G.Q. (2008). Disease-specific induced pluripotent stem cells. Cell *134*, 877–886.

Protze, S.I., Liu, J., Nussinovitch, U., Ohana, L., Backx, P.H., Gepstein, L., and Keller, G.M. (2016). Sinoatrial node cardiomyocytes derived from human pluripotent cells function as a biological pacemaker. Nat. Biotechnol. *35*, 56–68.

Reubinoff, B.E., Pera, M.F., Fong, C.-Y., Trounson, A., and Bongso, A. (2000). Embryonic stem cell lines from human blastocysts: somatic differentiation in vitro. Nat. Biotechnol. *18*, 399–404.

Shelton, M., Metz, J., Liu, J., Carpenedo, R.L., Demers, S.-P., Stanford, W.L., and Skerjanc, I.S. (2014). Derivation and expansion of PAX7-positive muscle progenitors from human and mouse embryonic stem cells. Stem Cell Reports *3*, 516–529.

Shelton, M., Kocharyan, A., Liu, J., Skerjanc, I.S., and Stanford, W.L. (2016). Robust generation and expansion of skeletal muscle progenitors and myocytes from human pluripotent stem cells. Methods *101*, 73–84.

Soldner, F., Hockemeyer, D., Beard, C., Gao, Q., Bell, G.W., Cook, E.G., Hargus, G., Blak, A., Cooper, O., Mitalipova, M., et al. (2009). Parkinson's disease patient-derived induced pluripotent stem cells free of viral reprogramming factors. Cell *136*, 964–977.

Takahashi, K., Tanabe, K., Ohnuki, M., Narita, M., Ichisaka, T., Tomoda, K., and Yamanaka, S. (2007). Induction of pluripotent stem cells from adult human fibroblasts by defined factors. Cell *131*, 861–872.

Tatsumi, R., Suzuki, Y., Sumi, T., Sone, M., Suemori, H., and Nakatsuji, N. (2011). Simple and highly efficient method for production of endothelial cells from human embryonic stem cells. Cell Transplant. *20*, 1423–1430.

Teo, A.K.K., Ali, Y., Wong, K.Y., Chipperfield, H., Sadasivam, A., Poobalan, Y., Tan, E.K., Wang, S.T., Abraham, S., Tsuneyoshi, N., et al. (2012). Activin and BMP4 synergistically promote formation of definitive endoderm in human embryonic stem cells. Stem Cells *30*, 631–642.

Thomson, J.A., Itskovitz-Eldor, J., Shapiro, S.S., Waknitz, M.A., Swiergiel, J.J., Marshall, V.S., and Jones, J.M. (1998). Embryonic stem cell lines derived from human blastocysts. Science *282*, 1145–1147.

Toh, W.S., Guo, X.M., Choo, A.B., Lu, K., Lee, E.H., and Cao, T. (2009). Differentiation and enrichment of expandable chondrogenic cells from human embryonic stem cells in vitro. J. Cell. Mol. Med. *13*, 3570–3590.

Touboul, T., Hannan, N.R.F., Corbineau, S., Martinez, A., Martinet, C., Branchereau, S., Mainot, S., Strick-Marchand, H., Pedersen, R., Di Santo, J., et al. (2010). Generation of functional hepatocytes from human embryonic stem cells under chemically defined conditions that recapitulate liver development. Hepatology *51*, 1754–1765.

Wu, S.M., and Hochedlinger, K. (2011). Harnessing the potential of induced pluripotent stem cells for regenerative medicine. Nat. Cell Biol. *13*, 497–505.

Yu, J., Vodyanik, M.A., Smuga-Otto, K., Antosiewicz-Bourget, J., Frane, J.L., Tian, S., Nie, J., Jonsdottir, G.A., Ruotti, V., Stewart, R., et al. (2007). Induced pluripotent stem cell lines derived from human somatic cells. Science *318*, 1917–1920.

Stem Cell Reports, Volume *13*

Supplemental Information

Transcriptomically Guided Mesendoderm Induction of Human Pluripotent Stem Cells Using a Systematically Defined Culture Scheme

Richard L. Carpenedo, Sarah Y. Kwon, R. Matthew Tanner, Julien Yockell-Lelièvre, Chandarong Choey, Carole Doré, Mirabelle Ho, Duncan J. Stewart, Theodore J. Perkins, and William L. Stanford

Figure S1. BMP4 and Activin A dose-response and mesendoderm differentiation of H1 and H7 hESCs. Related to Figure 1.

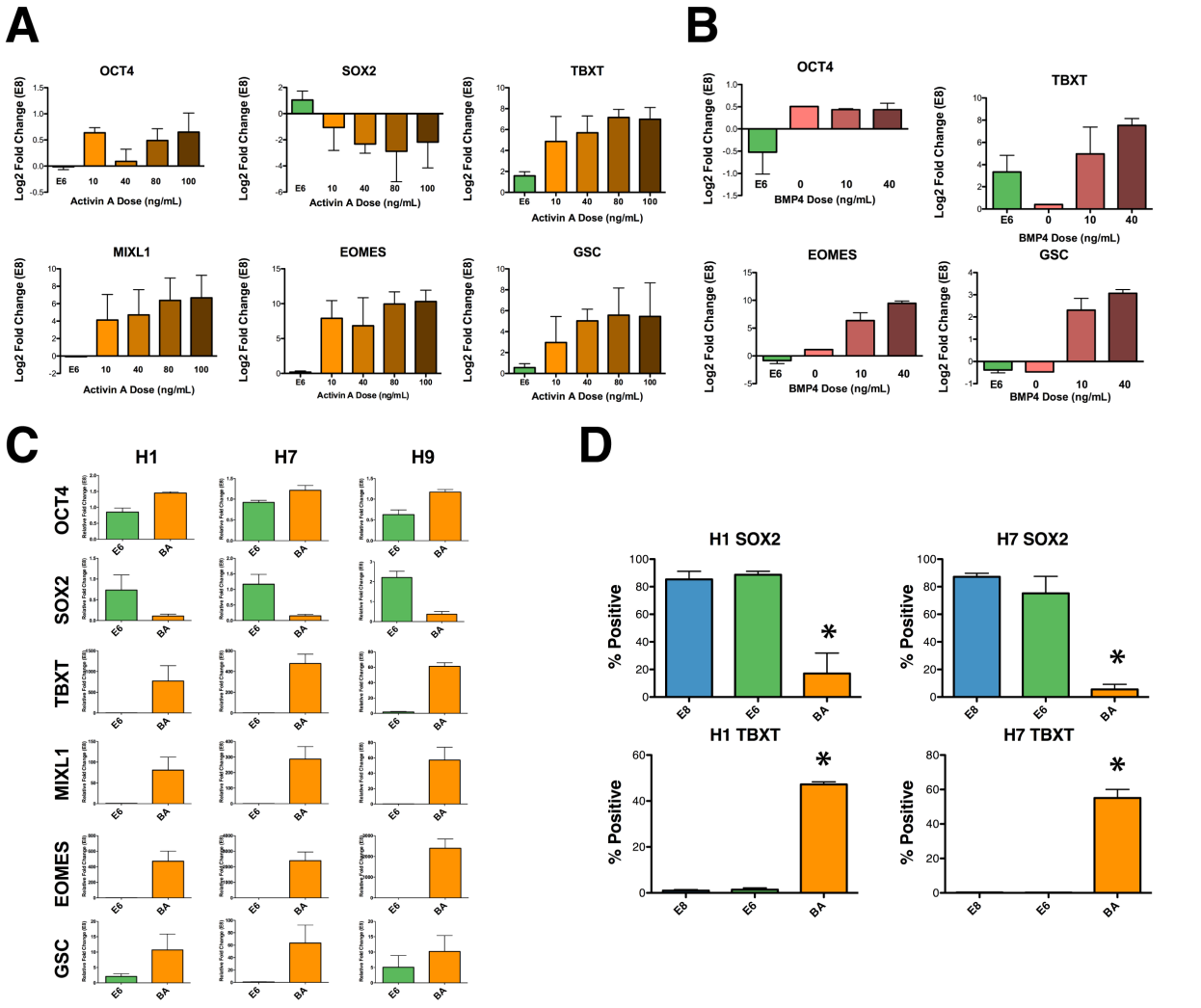

(A). Activin A dose was varied from 10-100 ng/mL with a constant BMP4 dose of 40 ng/mL. No significant difference in mesendoderm gene expression was observed at increasing Activin A dosage. (B). BMP4 dose was varied from 0-40 ng/mL with Activin A concentration of 40 ng/mL. (C). Single-cell seeding, BA treatment was performed for H1 and H7 hESCs as well as H9s, demonstrating similar trends in gene expression for all three lines. (D) Analysis of protein expression by immunofluorescence and high-content imaging likewise demonstrated similar loss of SOX2 and up-regulation of TBXT among all hESCs examined. Error bars represent SEM, n=3, *=$p<0.05$.

Figure S2. Co-expression of genes in 48-hour BA cells by single-cell gene expression analysis. Related to Figure 4.

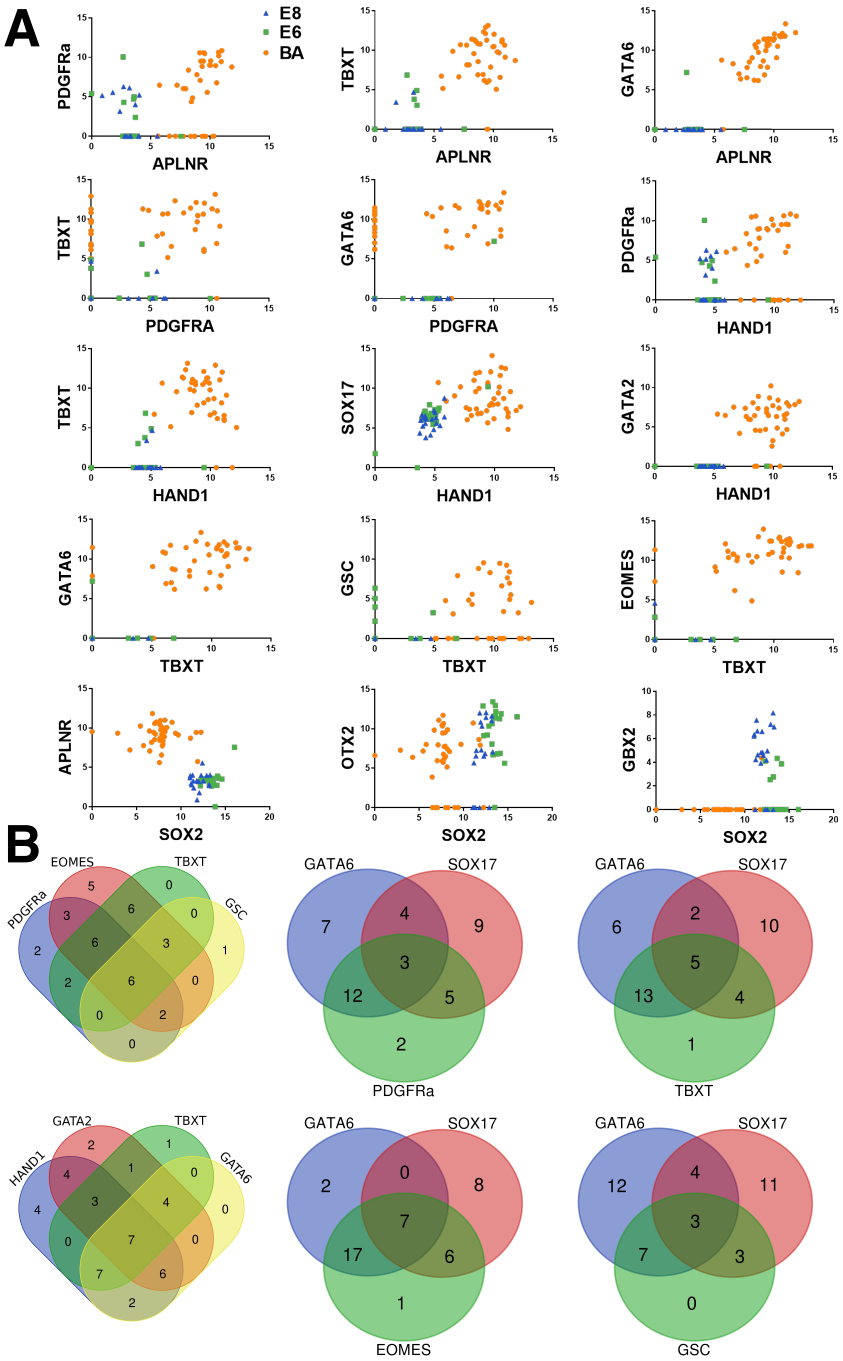

(A). Relative expression values of mesoderm and endoderm genes were plotted to assess co-expression in individual cells in BA (orange), E6 (green) and E8 (blue) cells, demonstrating the co-expression of many of these in the BA cells. Co-expression of *SOX2* with *OTX2* or *GBX2* separates E6 and E8 cells from BA cells (bottom row). (B) Venn diagrams depicting the overlap in cells with positive expression of mesoderm and endoderm genes in the BA population. Notable overlap was observed for expression of all genes examined, and expression of endoderm genes (*SOX17, GATA6*) was not able to identify a unique population that did not also express mesoderm genes.

Figure S3. Definitive endoderm differentiation of H1 and H7 hESC lines. Related to Figure 5.

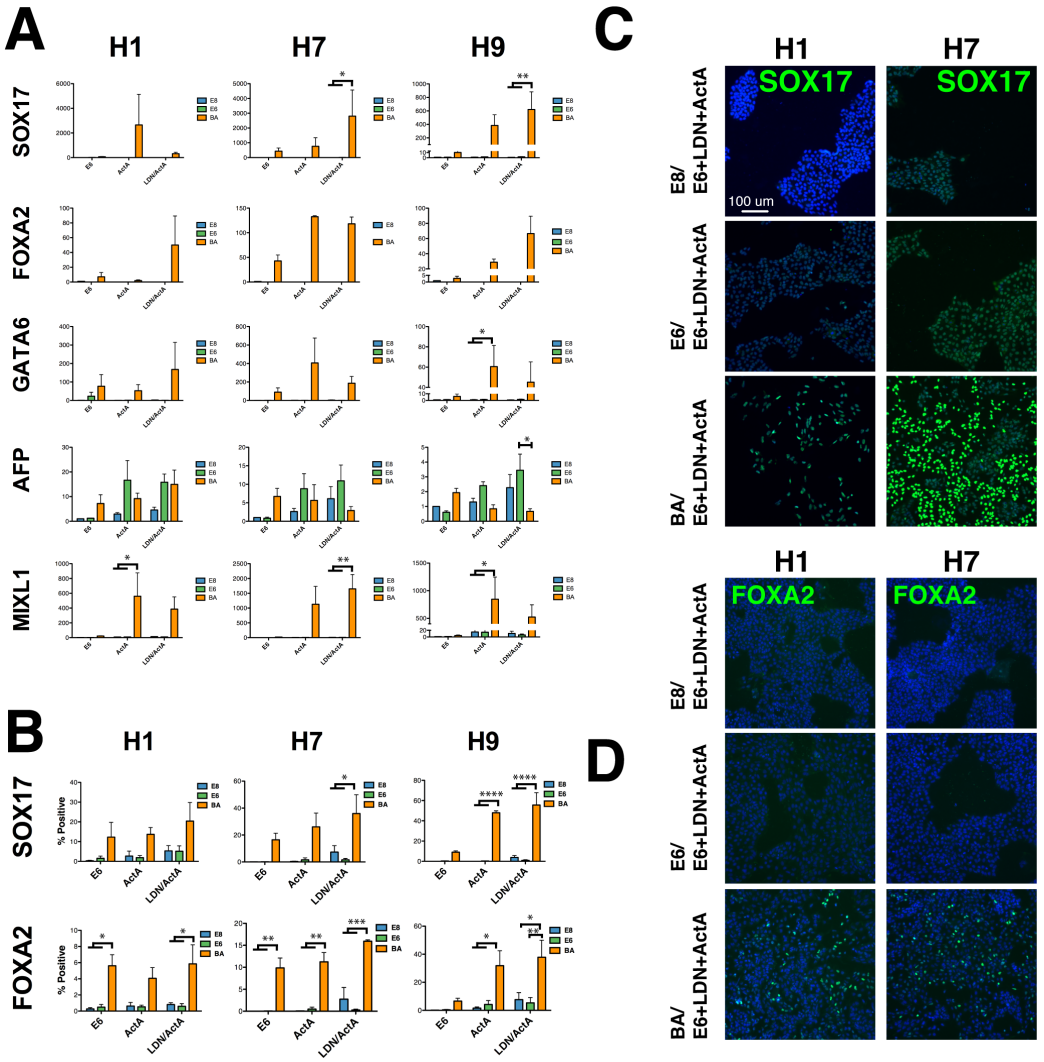

(A). Gene expression analysis in response to definitive endoderm conditions for cells pre-differentiated in E8 (blue bars), E6 (green bars) or BA (orange bars). Similar trends were observed in H1and H7 hESCs compared to H9s. (B). Analysis of SOX17 and FOXA2 protein expression, based on immunofluorescence, with representative images in panel (C). Expression of SOX17 and FOXA2 was highest in BA pre-differentiated cells in Activin A/LDN secondary media. Errors bars represent SEM, n=3, *=p<0.05, **=p<0.01, ***=p<0.001, ****=p<0.0001. Scale bar represents 100 µm.

Table S2. List of probes used for single-cell qPCR analysis. Related to Figure 4.

ACTB	CHAT	FGF5	GBX2	ITGB4	NANOG	POU4F2	SLC2A2
ALB	COL10A1	FOXA1	GDF3	KRT10	NESTIN	POU5F1	SLC32A1
APLNR	COMP	FOXD3	GFAP	KRT14	NEUROD1	PROM1	SMTN
APOH	CPA1	FOXG1	GSC	KRT19	NEUROG2	PTCRA	SOX17
AQP1	CTSK	G6PC	HAND1	LEFTY1	NKX2-2	RCVRN	SOX2
B2M	DCN	GAD1	HAND2	MAP3K12	NKX2-5	RPLP0	SOX7
BMP4	DCX	GAD2	HES5	MIOX	NPPA	RUNX1	T
CCR5	DNMT3B	GALC	HNF4A	MIXL1	OLIG2	RYR2	TAT
CD34	DPP4	GAPDH	HPRT1	MSLN	OTX2	SFTPB	TUBB3
CD3E	ENO1	GATA1	IBSP	MYH1	PAX6	SFTPD	TYR
CD79A	EOMES	GATA2	IGF2	MYH7	PDGFRA	SLC17A6	ZFP42
CER1	FABP7	GATA6	INS	MYL3	PODXL	SLC17A7	ZIC1

Table S3. Primer sequences used in qPCR gene expression analysis. Related to Figures 1, 5 and 6.

Gene	Forward Sequence	Reverse Sequence
OCT4	TCAGCCAAACGACCATCTGCCG	AGCAAGGGCCGCAGCTTACA
SOX2	TACAGCATGTCCTACTCGCAG	GAGGAAGAGGTAACCACAGGG
Nanog	ACGCAGAAGGCCTCAGCACCTA	AGGTTCCCAGTCGGGTTCACCA
T	ACCTGTGTCGCCACCTTCCA	ACCACTGGCTGCCACGACAA
MIXL1	TCCTCAACCACTGTGCTCCTGG	AACCCCGTTTGGTTCGGGCA
EOMES	AGGCGCAAATAACAACAACACC	ATTCAAGTCCTCCACGCCATC
GSC	CGCGGGACACTTGCCCGTATTA	AAGGCAGCGCGTGTGCAAGA
PAX6	CCAGAAAGGATGCCTCATAAA	TCTGCGCGCCCCTAGTTA
Nestin	CCGCATCCCGTCAGCTGGAAAA	GCTTGGGCACAAAAGCCAGCA
OTX2	CTTAAGCAACCGCCTTACGC	AGGGGTGCAGCAAGTCCATA
AFP	AGCTGACCTCGTCGGAGCTGAT	TCCCTCGCCACAGGCCAATAGT
KDR	ACCGTTAAGCGGGCCAATGGA	ACCACGGCCAAGAGGCTTACCT
SOX17	CGCACGGAATTTGAACAGTA	GGATCAGGGACCTGTCACAC
FOXA2	GGGAGCGGTGAAGATGGA	TCATGTTGCTCACGGAGGAGTA
GATA6	AGGCTGCAGTTTTCCGGCAGAG	CGCCGCGCTGCTGGTGAATAAA
GAPDH	TTCTTTTGCGTCGCCAGCCG	TGACCAGGCGCCCAATACGA
EF1a	GCTGGCTTCACTGCTCAGGTGATT	TGCAATGTGAGCCGTGTGGCA

Supplemental Experimental Procedures

Spatial Analysis

Spatial analysis for cells seeded as colonies at different split ratios or single-cells at different densities was performed using the SpatStat package for R (Baddeley and Turner, 2005; Baddeley et al., 2015). The spatial coordinates of each cell within a field (i.e. each microscopic image) were converted into a spatial point pattern, and each field was divided into 5x5 grids (totaling 25 quadrats). The number of points (or cells) per quadrat was quantified using the 'quadratcount' feature in Spatstat for each quadrat in each image acquired for a given well. The Coefficient of Variation (CV; standard deviation divided by mean) was then calculated for the number of cells per quadrat for each seeding condition. For each well, the total number of cells was quantified, and normalization of CV values was performed by calculating the CV of a simulated random uniform distribution of points (equal to the cell number in that well) using the 'runifpoint' function in Spatstat.

Bioinformatics

FASTQ sequencing data for each sample was aligned to GENCODE version 23 human genome annotations (hg38), using the HISAT2 alignment tool (version 2.0.1) (Kim et al., 2015). The 'featureCounts' function from the Rsubread package (version 1.22.3) (Liao et al., 2019)was used to count reads per gene, which were passed onto DESeq2 (version 1.12.4) (Love et al., 2014)for library size normalization and detection of differentially expressed genes (FDR <= 0.05). Hierarchical clustering was done with the R 'heatmap.2' function from the gplots package (version 2.17.0) for differentially expressed genes. Principal component analysis was done using an in-house R script and the built-in R PCA function 'prcomp'. Temporal expression path clustering was generated by unsupervised hierarchical clustering a log2 fold (log2FC) change matrix using R's built-in 'hclust' function. This was done for all genes with an absolute log2FC of at least 2 in any single timepoint. Clusters which were visibly similar were then manually combined, and cluster trajectories were then plotted using an in-house R script. Gene set enrichment analyses (Subramanian et al., 2005) were conducted by comparing differentially expressed genes from RNA-seq data to custom Gene Sets produced in-house. The -log10(p-value) for each gene from RNA-seq data was used as a custom weighting when GSEA analysis was conducted (version 2.1.0). Gene ontology analysis was performed using DAVID version 6.8 (Huang et al., 2009) and the BINGO plugin for Cytoscape (Maere et al., 2005).

Single-cell Gene Expression Analysis

Cycle numbers to enrichment for each gene in each cell were normalized to housekeeping genes between cells. Normalized cycle numbers were converted to a cycle difference measurement, subtracting observed cycle number from the mean cycle number of the corresponding gene across all cells. An aggregate vector of all cycle differences was used to produce Z-scores for each gene in each cell; these Z-scores were then used to plot heatmaps, using the R 'heatmap.2' function from the gplots package (version 2.17.0). t-SNE plots were also produced from cycle differences using the Rtsne package (version 0.10) and an in-house script for plotting the results. Tissue and cell type enrichment for single cell expression data was done using Enrichr (Chen et al., 2013; Kuleshov et al., 2016).

Chondrocyte Micromass Differentiation and Analysis

Following 48-hour pre-differentiation in E8, E6 or BA, cells (H9 hESCs or iPSCs) were dissociated using TrypLE Express and resuspended in chondrogenic media supplemented with 10 μM Y-27632. Chondrogenic media consisted of high glucose DMEM (Life Technologies) containing 1% KOSR, 1% ITS+ premix (BD Biosciences), 1% Sodium Pyruvate, 1% non-essential amino acids, 1% Penicillin-Streptomycin (Life Technologies), 100 μg/mL ascorbic acid 2-phosphate, 10^{-7} M dexamethasone, and 40 μg/mL L-proline (Sigma). Cells were resuspended at a density of $2x10^7$ cells/mL and plated as 15 μL drops in Matrigel-coated 12-well plates for 2 hours, after which 1 mL of chondrogenic media containing Y-27632 was added. Fresh chondrogenic media was added daily for course of the 7-day protocol.

To assess differentiation by matrix production, 4-5 micromass cultures were pooled and digested overnight at 65°C using 40 μg/mL papain enzyme in digestion buffer and processed for quantification as described (Lee et al., 2011). Sulfated glycosaminoglycan (s-GAG) content was quantified using Dimethylmethylene blue (DMMB). Hydroxyproline (OH-Pro) content was quantified by acid hydrolysis of papain-digested samples followed by neutralization, oxidation, and addition of 4-dimethylaminobenaldehyde. Hoechst 33258 dye was used to quantify DNA content in the samples, and total s-GAG or OH-Pro content were normalized to amount of DNA. Proteoglycan production was assessed after 7 days by Alcian Blue staining. Micromass cultures were fixed in 4% PFA for 15 min, rinsed with 0.2N HCl, and stained with 0.1% Alcian Blue solution at pH1 (diluted with 0.2N HCl from 0.3% w/v Alcian blue in 70% ethanol solution; Sigma) overnight at room temperature. Cultures were rinsed thoroughly with distilled water and imaged using a Zeiss Axio Zoom V16.

Endothelial Progenitor Cell Differentiation and Analysis

Differentiation of iPSCs derived from late-EPCs (described in Chang et al., 2013) was performed using an adapted protocol from Tatsumi *et al* (Tatsumi et al., 2011). Briefly, cells were pretreated for 48 hours with E6 supplemented with 10 ng/ml of both BMP4 and Activin A. Subsequently, cells were cultured in DMEM/F12 (Life Technologies) supplemented with B27 (Life Technologies), N2 (Life Technologies) and BIO (Sigma) for 72 hours with daily media change performed. Cells were then cultured in StemPro-34 (Life Technologies) supplemented with 50 ng/ml of $VEGF_{165}$ (R&D Systems) for a further 48 hours prior to MAC-selection with CD144

microbeads (Miltenyi Biotech). CD144 enriched cells were then further expanded and routinely passaged in StemPro-34 media supplemented with 50 µg/ml $VEGF_{165}$.

Endothelial cell differentiation was assessed by flow cytometry against a panel of endothelial cell surface markers. Briefly, following six days of differentiation, cells were harvested and dissociated into single cell suspension using TrypLE. A total of 2 $x10^5$ cells in 200 µl of flow buffer was enumerated and aliquotted into each tube. Directly conjugated antibodies (all from BD Bioscience) to CD31 (Cat. No. 340297), CD34 (Cat. No. 345802), CD45 (Cat. No. 555482), CD144 (Cat. No. 560411) and VEGFR (Cat. No. 560494) were then added at the recommended manufacturer's dilution into each tube (i.e. 20 µl per test) and incubated on ice in the dark for 30 mins. To halt the staining process, 400 µl of flow buffer was added per tube and the entire volume of 600 µl was subjected to centrifugation at 400rpm for 5 mins. Supernatant was decanted and cells resuspended in 300 µl flow buffer prior to analysis on an Attune acoustic focus cytometer (Life Technologies). To gate samples for FACS analysis, cells (20,000 events) were initially gated by FSC-A vs SCS for the exclusion of debris. Data were analyzed using FlowJo v10.0.6 software.

Definitive Endoderm Differentiation and Analysis

Pre-differentiation of H1, H7 or H9 hESCs was performed by SCS in E8, E6 or BA as described in the main text. For endoderm induction, BMP4 and Activin A concentration were adjusted to 10 and 60 ng/mL, respectively. After 48 hours in pre-differentiation conditions (E8, E6, BA), media was replaced with E6 alone, E6 with high Activin A concentration (100 ng/mL) or E6 with Activin A (100 ng/mL) and LDN193189 (250 nM). Cells were allowed to differentiate for an additional 48 hours, with media refreshed daily. Analysis of definitive endoderm induction was performed by immunostaining and high-content imaging of SOX17 and FOXA2, as well as gene expression of *SOX17, FOXA2, AFP*, and *GATA6*.

Neural Induction

Single-cell seeding and 48-hour differentiation in E8, E6 or BA was performed as described above. After 48 hours, media was aspirated and replaced with either fresh E6 or E6 supplemented with 10µM SB431542 and 100 nM LDN193189. Media was replaced daily for 3 additional days of differentiation. At the 48-hour and 5-day time points, RNA samples were collected for gene expression analysis, and wells were fixed in 4% PFA for immunofluorescent imaging.

Teratoma Formation and Analysis

Cells pre-differentiated in E8, E6 or BA were dissociated by TrypLE, and $1.0x10^6$ cells were embedded in Matrigel and injected into the tibialis anterior muscles of *NOD/SCID* mice (Charles River Laboratory). These procedures were approved by the University of Ottawa Animal Care Veterinary Services (protocol #OHRIT-1666). Tumors were allowed to form for 9-18 weeks before teratomas were excised, fixed in 4% formaldehyde, and embedded in paraffin. Paraffin-embedded teratomas were sectioned and stained with hematoxylin and eosin (H&E) or by immunofluorescence (IF). For IF, sodium citrate/pressure cooker antigen retrieval was performed. Slides were blocked and permeabilized in 2% BSA, 0.01% Triton X-100 prior to overnight primary antibody incubation at 4°C. Details for SOX2, SOX17 and Desmin antibodies can be found in Supplemental Methods. Secondary antibodies were added for 1 hour at room temperature (AlexaFluor 680 or 488, 1:400). Nuclei were stained with Hoechst 33342 for 15 minutes prior to coverslipping. Imaging of H&E sections was performed using an Aperio CS2 scanscope (Leica Biosystems), and IF sections were imaged using the Cellomics ArrayScan. Quantification of cartilage regions in H&E sections and positive staining in IF was performed using custom scripts written for ImageJ.

Primary Antibodies

OCT4A (Cell Signaling Technology C52G3; 1:400), Brachyury T (R&D Systems AF2085, 5 µg/mL), SOX2 (R&D Systems MAB2018, 8 µg/mL; EMD Millipore AB5603, 1:200), Nestin (EMD Millipore ABD69, 1:500), Desmin (Abcam ab191181, 1:200) and SOX17 (R&D Systems AF1974, 1:100).

Supplemental References

Baddeley, A., and Turner, R. (2005). **spatstat** : An *R* Package for Analyzing Spatial Point Patterns. J. Stat. Softw.

Baddeley, A., Rubak, E., and Turner, R. (2015). Spatial Point Patterns: Methodology and Applications with {R} (London: Chapman and Hall/CRC).

Chang, W.Y., Lavoie, J.R., Kwon, S.Y., Chen, Z., Manias, J.L., Behbahani, J., Ling, V., Kandel, R.A., Stewart, D.J., and Stanford, W.L. (2013). Feeder-independent derivation of induced-pluripotent stem cells from peripheral blood endothelial progenitor cells. Stem Cell Res. *10*, 195–202.

Chen, E.Y., Tan, C.M., Kou, Y., Duan, Q., Wang, Z., Meirelles, G., Clark, N.R., and Ma'ayan, A. (2013). Enrichr: interactive and collaborative HTML5 gene list enrichment analysis tool. BMC Bioinformatics *14*, 128.

Huang, D.W., Sherman, B.T., and Lempicki, R.A. (2009). Systematic and integrative analysis of large gene lists using DAVID bioinformatics resources. Nat. Protoc. *4*, 44–57.

Kim, D., Langmead, B., and Salzberg, S.L. (2015). HISAT: a fast spliced aligner with low memory requirements. Nat. Methods *12*, 357–360.

Kuleshov, M. V, Jones, M.R., Rouillard, A.D., Fernandez, N.F., Duan, Q., Wang, Z., Koplev, S., Jenkins, S.L., Jagodnik, K.M., Lachmann, A., et al. (2016). Enrichr: a comprehensive gene set enrichment analysis web server 2016 update. Nucleic Acids Res. *44*, W90-7.

Lee, W.D., Hurtig, M.B., Kandel, R.A., and Stanford, W.L. (2011). Membrane Culture of Bone Marrow Stromal Cells Yields Better Tissue Than Pellet Culture for Engineering Cartilage-Bone Substitute Biphasic Constructs in a Two-Step Process. Tissue Eng. Part C Methods *17*, 939–948.

Liao, Y., Smyth, G.K., and Shi, W. (2019). The R package Rsubread is easier, faster, cheaper and better for alignment and quantification of RNA sequencing reads. Nucleic Acids Res.

Love, M.I., Huber, W., and Anders, S. (2014). Moderated estimation of fold change and dispersion for RNA-seq data with DESeq2. Genome Biol. *15*, 550.

Maere, S., Heymans, K., and Kuiper, M. (2005). BiNGO: a Cytoscape plugin to assess overrepresentation of gene ontology categories in biological networks. Bioinformatics *21*, 3448–3449.

Subramanian, A., Tamayo, P., Mootha, V.K., Mukherjee, S., Ebert, B.L., Gillette, M.A., Paulovich, A., Pomeroy, S.L., Golub, T.R., Lander, E.S., et al. (2005). Gene set enrichment analysis: a knowledge-based approach for interpreting genome-wide expression profiles. Proc. Natl. Acad. Sci. U. S. A. *102*, 15545–15550.

Tatsumi, R., Suzuki, Y., Sumi, T., Sone, M., Suemori, H., and Nakatsuji, N. (2011). Simple and highly efficient method for production of endothelial cells from human embryonic stem cells. Cell Transplant. *20*, 1423–1430.